Toward broadband vibration-based energy harvesting

Tang, Lihua; Yang, Yaowen; Soh, Chee Kiong

2010

Tang, L., Yang, Y., & Soh, C. K. (2010). Toward broadband vibration-based energy harvesting. Journal of intelligent material systems and structures, 21(18), 1867-1897.

https://hdl.handle.net/10356/99680

https://doi.org/10.1177/1045389X10390249

Towards Broadband Vibration-based Energy Harvesting

Lihua TANG [1], Yaowen YANG [2*] and Chee Kiong SOH [3]

[1,2,3] School of Civil and Environmental Engineering,

Nanyang Technological University, 50 Nanyang Avenue, Singapore 639798

[2*] Corresponding author, cywyang@ntu.edu.sg; [1] lihuatang@pmail.ntu.edu.sg;
[3] csohck@ntu.edu.sg

ABSTRACT

The dramatic reduction in power consumption of current integrated circuits has evoked great research interests in harvesting ambient energy, such as vibrations, as a potential power supply for electronic devices to avoid battery replacement. Currently, most vibration-based energy harvesters are designed as linear resonators to achieve optimal performance by matching their resonance frequencies with the ambient excitation frequencies a priori. However, a slight shift of the excitation frequency will cause a dramatic reduction in performance. Unfortunately, in the vast majority of practical cases, the ambient vibrations are frequency-varying or totally random with energy distributed over a wide frequency spectrum. Hence, developing techniques to increase the bandwidth of vibration-based energy harvesters has become the next important problem in energy harvesting. This paper reviews the advances made in the past few years on this issue. The broadband vibration-based energy harvesting solutions, covering resonance tuning,

multimodal energy harvesting, frequency up-conversion and techniques exploiting nonlinear oscillations, are summarized in detail with regard to their merits and applicability in different circumstances.

Keywords: energy harvesting; vibration; broadband; resonant frequency; nonlinear oscillation

1 INTRODUCTION

With the advances in integrated circuits, the size and power consumption of current electrical applications have dramatically decreased. For example, a wireless sensor can be powered at as low as 100μW. Currently, the portable devices and wireless sensing applications are powered by batteries. However, as shown in Figure 1, the improvement of battery energy density remains stagnant as compared with the other computing hardware (Anton and Sodano, 2007; Paradiso and Starner, 2005). Besides, with battery included in the application means not only tedious and expensive replacement cost but also limitation on its miniaturization. Hence, in the past few years, ambient energy harvesting as power supply for low-scale electronics has evoked great research interests from various academic communities, including material science, mechanical, civil and electrical engineering.

Different energy sources existing in the environment around a system, such as sunlight, wind, thermal gradient and mechanical vibration, can be the options for energy

harvesting. Among them, the vibration sources can be found almost everywhere in our daily life (as shown in Table 1) and hence have attracted much research attention. Current solutions for vibration-to-electricity conversion are mostly accomplished via electrostatic (Roundy et al., 2003; Micheson et al., 2004), electromagnetic (El-Hami et al., 2001; Micheson et al., 2004) or piezoelectric principles (Yang et al., 2009). Various models, including analytical models (Erturk and Inman, 2008a; Micheson et al., 2004), finite element models (De Marqui et al., 2009; El-Hami et al., 2001) and equivalent circuit models (Yang and Tang, 2009), have been established to investigate the energy harvesting capability of each principle. No matter which principle was exploited, most of the previous research work focused on designing a linear vibration resonator, in which the maximum system performance can be achieved when the energy harvester is tuned to match its resonance frequency with the external excitation frequency. If the excitation frequency slightly shifts, the performance of the harvester will dramatically decrease. Since in the majority of practical cases, the vibration in the environment is frequency-varying or totally random with the energy distributed in a wide spectrum, how to broaden the bandwidth of harvesters becomes one of the most challenging issues before their practical deployment.

This article presents a review of the recent advances in broadband vibration-based energy harvesting. The state-of-the-art techniques in this field, covering resonance frequency tuning techniques, multimodal energy harvesting, frequency up-conversion and techniques exploiting nonlinear oscillations, are summarized in detail with regard to their merits and applicability in different circumstances.

2 RESONANCE FREQUENCY TUNING TECHNIQUES

In most of the reported studies, the energy harvesters are designed as linear resonators to match their resonance frequencies with the excitation frequencies to achieve optimal power output. The geometry and dimensions of the harvester can be carefully selected for frequency matching when the excitation frequency is known a priori. However, when the excitation frequency is unknown or varies in different operational conditions, the energy harvester with fixed resonance frequency may not be able to achieve optimal power output. Hence, in practice, an energy harvester is expected to incorporate a resonance tuning mechanism to increase its functionality. According to Roundy and Zhang (2005), the resonance can be tuned 'actively' or 'passively'. Active mode requires continuous power input for resonance tuning. While in passive mode, intermittent power is input for tuning and no power required when frequency matching is completed, until the excitation frequency varies again. According to different tuning mechanism, the resonance tuning methods can also be categorized into mechanical, magnetic and piezoelectric methods. In this section, the recent techniques using the above methods are reviewed and summarized.

2.1 Mechanical methods

From the viewpoint of vibration theory, the resonance of a system can be tuned by changing the stiffness or mass. Usually, it is more practical to change the stiffness rather than the mass of the system. Leland and Wright (2006) presented one technique to tune the resonance of their harvester by applying an axial compressive load, which actually

altered the stiffness of the harvester. Figure 2 shows the schematic of a simply supported bimorph energy harvester with applied preload. In their experimental test on the prototype, it was determined that before bimorph failure, a compressive axial preload can reduce the resonance frequency of a vibration energy scavenger by up to 24% while simultaneously increasing the damping, as shown in Figure 3. For their prototype with a 7.1g proof mass attached under the excitation of 1g acceleration, 300~400μW can be obtained over the range of 200~250Hz. The design presented was intended to operate in 'passive' mode, where the device should be manually tuned. However, the energy required for the tuning procedure was not addressed by Leland and Wright (2006). Furthermore, the resonance frequency can only be tuned uni-directionally.

Eichhorn et al. (2008) conducted a similar study on resonance frequency shift by using prestress. A cantilevered tunable energy harvester was designed and fabricated. Figure 4 shows the generator and the schematic of the entire setup. Two wings connected the tip of the beam and the arms. The revolution of the screw generated the compression on the spring, which applied the force on the arms. The force was then forwarded by the wings and finally applied at the free end of the cantilever. Below the fracture limit, a resonance shift from 380Hz to 292Hz was achieved by applying up to 22.75N preload, as shown in Figure 5. The quality factor was reduced, which means damping arose with increased preload. Furthermore, the harvester should be tuned manually and the automatic controller for tuning procedure was not implemented in their design.

Analytically, Hu et al. (2007) derived the governing equations of a cantilever

piezoelectric bimorph with an axial preload and investigated its feasibility and characteristics of resonance. The resonance can be adjusted either higher or lower with a tensile or compressive load, respectively. In their model, it was reported that a tensile load F_a = -50N increased the resonance from 129.3 to 169.4Hz while a compressive load F_a = 50N decreased the resonance from 129.3 to 58.1Hz.

Rather than bending mode, some researchers also investigated the tunable resonator working in extensional mode, termed XMR (Morris et al., 2008; Youngsman et al., 2010). The XMR presented by Morris et al. (2008) was formed by suspending a seismic mass with two piezoelectric membranes (PVDF). Pre-tensioning two rectangular membranes (with dimensions of $2l \times w \times h$ and Young's modulus E) by a rigid link with length of $2u_p$ and deflecting the link by Δu, as shown in Figure 6, the force–deflection characteristics of the rigid link was found to be

$$F = \frac{Ewh}{l^3}\left(6u_p^2\Delta u + 2\Delta u^3\right) \tag{1}$$

Figure 7 shows the normalized force–displacement relationship of Eqn. (1). For sufficiently small deflection, the natural frequency can be approximated as

$$f_N = \frac{1}{2\pi}\sqrt{\frac{k}{m}} = \frac{1}{2\pi}\sqrt{\frac{dF}{d(\Delta u)}\Big/ m} \approx u_p \frac{1}{2\pi}\sqrt{6\frac{Ewh}{ml^3}} \tag{2}$$

Hence, the resonance frequency can be tuned by adjusting the link length that symmetrically pre-tensions both piezoelectric sheets. Similar force-deflection relationships and natural frequency expressions can be found for other rigidly coupled and transversely loaded membrane. For the fabricated XMR prototype with circular

configuration (Figure 8), the frequency response functions were obtained by tuning the preloading screw at three random adjustment positions as shown in Figure 9. Apparently, from Figure 9, the resonance frequency was repeatable when the tuning screw was repositioned to the same position. It was found that for the devised prototype, the resonant frequency shift between 80 and 235 Hz can be easily achieved with the change of pre-tension displacement of around 1.25mm. Morris et al. (2008) claimed that this was not the upper limit of their XMR, which would be determined by the mechanical failure. However, the ability to self-tune or sequentially tune during operation of the XMR was not investigated.

A similar investigation was pursued by Loverich et al. (2008), in which the resonance can be tuned by adjusting the pre-deflection of the circular plate, as shown in Figure 10. The resonance frequency could be experimentally varied between 56 and 62Hz by adjusting the boundary location by approximately 0.5mm. More than its tunability, they also focused on the nonlinearities of the pre-deflected plate. Similar nonlinear force-deflection characteristics were obtained as Eqn. (1). The benefit of the nonlinear stiffness system was that the resonance frequency and system quality factor Q were dependent on the periodic deflection of the stiffness elements. The stiffness was nearly linear and the system had a high Q for low vibration amplitudes, while the resonance frequency shifted and Q was reduced for high vibration amplitudes. This feature of nonlinear stiffness was claimed an auto protection mechanism, which is important for applications where high sensitivity is required for low vibration levels but mechanical robustness is required for high vibration levels.

Rather than applying the axial or in-plane preload, adjusting the gravity center of the tip mass is another idea to adjust the resonance of a cantilever. Wu et al. (2008) presented such a cantilevered energy harvester by realizing a movable tip mass. The proof mass consisted of a fixed part and a movable part, as shown in Figure 11. The gravity center of the whole proof mass can be adjusted by driving the movable screw. The fixed part of mass was made of a material of relatively small density and the movable part material was of larger density such that the moving distance of the gravity center of proof mass and in turn the frequency tunability can be enlarged. In their prototype, the adjustable resonance frequency range could cover 130~180Hz by tuning the gravity center of the tip mass up to 21mm, as illustrated in Figure 12.

2.2 Magnetic methods

Applying magnetic force to alter the effective stiffness of the harvester is another option for resonance tuning. Challa et al. (2008) proposed such a tunable harvester as shown in Figure 13. Two magnets were fixed to the free end of the cantilever beam, while the other two magnets were fixed to the top and bottom of the enclosure of the device. All magnets were vertically aligned so that attractive and repulsive magnetic forces could be generated on each side of the beam. By tuning the distance between the magnets using a spring-screw mechanism, the magnetic force could be altered, which induced an additional stiffness on the beam and in turn adjusted its resonance frequency. The power output of the prototype device, with a volume of $50cm^3$, was reported to be 240~280μW operating at an acceleration amplitude of $0.8m/s^2$ over the frequency range of 22~32Hz.

Power output was undermined as the damping increased during the tuning procedure, as shown in Figure 14. Given the maximum tuning distance of 3cm, the required energy was 85mJ and it would take around 320s for each tuning procedure, which means the harvester can only work where the excitation frequency changes slowly. Besides, like the aforementioned designs, no 'smart' controller for resonance tuning process was implemented.

Reissman et al. (2009) also demonstrated a tuning technique using variable attractive magnetic force, as shown in Figure 15. With this design, the resonance of the piezoelectric energy harvester could be tuned bi-directionally by adjusting a magnetic slider mechanism. This is much simplified as compared with the design of Challa et al. (2008). The effective stiffness of the piezoelectric beam was dependent on the structural component K_m, the electromechanical component K_e that varied with external resistive loading R_l, and the magnetic stiffness $K_{magnetic}$ that varied with the relative distance D between the two magnets, i.e.,

$$K_{eff} = \left(K_m + K_e\left(R_l\right)\right) + K_{magnetic}\left(D\right) \tag{3}$$

According to the concept of a potential energy well, by tuning the vertical relative distance D_y of the two magnets, the resonance could be tuned bi-directionally, as shown in Figure 16. For a fixed D_x, the maximum frequency achieved was 99.38Hz, at $D_y = 0$, and the lowest frequency was 88Hz at $D_y = 1.5$cm, as shown in Figure 17. Hence, the total bandwidth of the harvester was 11.38Hz, including the resonance frequency shift from short-circuit to open-circuit condition due to the piezoelectric coupling.

Zhu et al. (2008) proposed a similar setup using magnets for resonance adjustment, but they further implemented a smart controller for tuning procedure. The linear actuator, as shown in Figure 18, adjusted the distance between the two magnets, tuning the attractive force and hence the resonance of the beam. The tuning process was controlled by a microcontroller, which woke up periodically, detected the output voltage of the generator and gave instructions to drive the actuator. In their experimental test, the resonant frequency could be tuned from 67.6 to 98Hz when the distance between the two magnets was changed from 5 to 1.2mm but it could not be further increased when the distance was smaller than 1.2mm, as shown in Figure 19. When excited at a constant acceleration level of 0.588m/s^2, a power of 61.6-156.6μW over the tuning range could be achieved, as shown in Figure 20. Additionally, they found that the damping of the micro-generator was not affected by the tuning mechanism over most of the tuning range. However, the damping was increased and the output power was less than expected if the tuning force became larger than the inertial force caused by vibration.

In their design, the energy consumed for the tuning procedure was 2.04mJ·mm^{-1}. They claimed that the linear actuator and microcontroller would be ultimately powered by the generator itself and the closed loop frequency tuning system would look like Figure 21. However, experimentally, the linear actuator and microcontroller were still powered by a separate power supply for preliminary evaluation. Another drawback of the control system they presented was that the system could be triggered by mistake if there were any change in the amplitude and phase of vibration.

2.3 Piezoelectric methods

A piezoelectric actuator can alter the stiffness of a system. In fact, the stiffness of the piezoelectric material itself can be varied with different electrical load attached. Hence, piezoelectric transducers provide another option for resonance tuning. It should be emphasized that the notion "piezoelectric methods" refers to the methods for resonance tuning using piezoelectric transducers. The energy generation method could be electrostatic, electromagnetic or piezoelectric conversion.

Wu et al. (2006) presented a piezoelectric bimorph generator in which the upper piezoelectric layer was used for tuning purpose by connecting various capacitive loads, while the lower layer for energy harvesting to charge a supercapacitor, as shown in Figure 22. The tunable bandwidth of the generator was 3Hz from 91.5 to 94.5Hz, which was much narrower than those achieved by the other aforementioned designs. In the two demo tests, the device was excited under a chirp and random vibration from 80 to 115Hz. When the real-time tuning system was turned on, the average harvesting power of 1.53mW and 1.95mW were generated respectively. These results corresponded to respective 13.4% and 27.4% increase as compared with the output when the tuning system was turned off. A microcontroller was utilized to sample the external frequency and adjusted the capacitive load to match the external vibration frequency in real-time, in other words, the device was tuned actively. The continuous power required by the microcontroller system was in μW level.

Peters et al. (2009) proposed another novel tunable resonator whose mechanical stiffness

and hence the resonance can be adjusted through two piezoelectric actuators. The free actuator swings around the axis of rotation with a deflection angle α, as shown in Figure 23(a). By applying a voltage on the actuators, both ends of the actuators will deflect by $\Delta y(V_{op})$, as shown in Figure 23(b). Such deformation will cause an additional hinge moment and thus a stiffer structure. For the large resonator they fabricated, a large tuning range of over 30% from an initial frequency of 78 Hz was achieved by using a tuning voltage of only ±5V, as shown in Figure 24. A discrete control circuit, which exploited the phase characteristic of the resonator, was implemented to actively control the resonance tuning. However, the power consumption of around 150mW was supplied externally, which significantly outweighed the harvested power (1.4mW). Thus, a low-power CMOS integration of the control circuit was recommended to be studied for practical close-loop automatic tuning.

Roundy and Zhang (2005) investigated the feasibility of active tuning mechanism. Via analytical study, they demonstrated that an 'active' tuning actuator never resulted in a net increase in power output, i.e., the power required to continuously tune the natural frequency always exceeded the power increase resulting from the frequency tuning. The fabricated piezoelectric generator, with an active tuning actuator, is shown in Figure 25. The electrode was etched to create a scavenging and a tuning part. Through three experimental test cases, it was found that the change in power output (82μW) as a result of tuning was significantly smaller than the power needed to continuously drive the actuator (440μW), which verified the conclusion of their analytical study. They suggested that 'passive' tuning mechanism was worth more attention.

Wischke et al. (2010) reported a design of tunable electromagnetic harvester in which the resonance was adjusted in a 'semi-passive' way. Figure 26 shows the schematic of the design. The maximum tunable frequency range covered 56Hz between 267 to 323Hz by applying the voltage -100V~+260V to the piezoelectric bimorph actuator. This was equivalent to 18% of the basic resonance frequency at an open circuit of 299Hz. More than 50μW with optimal resistive loading were continuously achieved across the tunable frequency range. However, once the control voltage was disconnected, the frequency drifted away from the initial adjusted value due to leakage of the piezoceramic, as shown in Figure 27. The drifting was more intense for high control voltages (>130V). The charge had to be refreshed periodically to maintain the desired resonance frequency. Hence, the tuning mechanism was defined as 'semi-passive' by Wischke et al. (2010) since it is different from the 'passive' principle, in which the charge on the piezoceramic and accordingly the adjusted frequency would remain constant after disconnecting the control voltage. In order to reduce the frequency drifting and the energy required for tuning, the tuning range was suggested to be limited to 25Hz by applying a voltage of -65~+130V, which was still feasible for sensor nodes. To further reduce the energy required for tuning, the shorter electrode of 10mm length was used, which could achieve 80% of the tuning range, i.e., 20Hz. Hence, given the power output of 50μW, 20% circuit efficiency and 200μJ required for tuning, the resonance frequency of the harvester could be tuned across 20Hz in every 20s.

2.4 Summary of resonance tuning methods

Table 2 compares the reported resonance tuning methods with regard to tunability (frequency change / average frequency), tuning load, tuning energy required and whether an automatic controller was implemented.

(1) *Mechanical methods.* From Table 2, generally, using mechanical tuning can achieve the largest tunability. However, all the tunable designs using mechanical method require manual adjustment of the system parameters, such as the preload or pre-deflection, and gravity center of the tip mass. Tuning screws are widely used in most of these adjusting procedures, which makes it difficult to implement automatic tuning during operation. The mechanical work required for tuning is not addressed in the literature reviewed.

(2) *Magnetic methods.* Using magnets for resonance tuning can achieve median tunability. Most of the reported designs still require manual tuning, but fortunately, it is relatively easier to implement the tuning mechanism than the reported mechanical methods, e.g., by adjusting the distance between the magnets using a piezoelectric actuator (Zhu et al., 2008). Thus, the tuning procedure can be automatically controlled and achieved during the operation of the harvester. However, the required energy of 2.04mJ·mm^{-1} for actuating the tuning procedure challenges its feasibility in practice. Furthermore, it should be mentioned that these magnetic methods introduce nonlinearity in the system. (This nonlinearity itself can also be exploited to broaden the bandwidth, which will be discussed in Section 5.) Similar to the nonlinear techniques described in Section 5, the drawback of the magnetic methods for

resonance tuning is that some harvested power will be consumed to perturb the system into the higher amplitude branch of the frequency response curve.

(3) *Piezoelectric methods.* As shown in Table 2, piezoelectric methods provide the smallest tunability as compared with the mechanical and magnetic methods. However, they are favorable for tuning during operation by applying voltage to the actuators (Peters et al., 2009; Roundy and Zhang, 2005; Wischke et al., 2010) or switching the electrical load (Wu et al., 2006). For the designs of Peters et al. (2009) and Roundy and Zhang (2005), the reported power required for active tuning outweighs the power generated from energy harvesting; while, Wu et al. (2006) reported that the power required is only in the μW level such that net power increase can be obtained. The reason for this difference is that the concept behind the design of Wu et al. (2006) is piezoelectric shunt damping where power is only required to continuously switch the electrical load to change the system stiffness, rather than applied to the actuator, which usually consumes more power. However, the shunt damping concept provides relatively low tunability, i.e., applicable to very narrow frequency bandwidth, as compared with the other piezoelectric tuning methods.

(4) *Active tuning versus passive tuning.* Active tuning is usually implemented by piezoelectric tuning methods. Generally, it requires more power input than passive tuning and outweighs the power generated in most of the reported designs except that of Wu et al. (2006). This limits their applicability in practice. On the other hand, passive tuning requires less power input to periodically detect and change the frequency, which is suitable when the excitation frequency varies slowly. However, if the harvested power can afford the continuous power required for tuning, an active

tuning harvester can work under excitation with fast-varying frequency or under random excitation, such as that of Wu et al. (2006).

3 MULTIMODAL ENERGY HARVESTING

In practice, the energy harvester is a multi-degree-of-freedom system or a distributed parameter system. Certain vibration mode can be excited when the driving frequency approaches one natural frequency of the harvester. If multiple vibration modes of the harvester are utilized, useful power can be harvested over multiple frequency spectra, i.e., wider bandwidth can be covered for efficient energy harvesting. Here, we term such techniques as 'multimodal energy harvesting'.

3.1 Hybrid energy harvesting scheme

In a given scenario, two different schemes can be combined in one system such that one assists the other for vibration energy harvesting, such as combining the piezoelectric and electromagnetic principles (Challa et al., 2009; MacCurdy et al., 2008; Tadesse et al., 2009). One example is the design of a multimodal energy harvester presented by Tadesse et al. (2009), as shown in Figure 28. The harvester consists of a cantilever beam with piezoelectric plates bonded and a permanent magnet attached at the tip, which oscillates within a stationary coil fixed to the housing. It was found that the electromagnetic scheme generated high output power at low frequency (first mode), while the piezoelectric scheme generated higher power at higher frequency (second mode). Hence, combination of the two schemes in one device could provide significant power output covering multiple frequency spectra. However, the first resonance and the second

resonance of such prototype were 20Hz and 300Hz, respectively, which means the discrete effective bandwidth may only be helpful when the excitation vibration has a rather wide frequency spectrum. The increased size may be another drawback since the permanent magnet is usually difficult to be reduced to small scale. Besides, there is a drastic difference in the magnitude of matching load for electromagnetic and piezoelectric cases, which presents difficulty in combining the output power from the two mechanisms thus requiring separate converter circuits.

3.2 Cantilever array

Rather than discrete bandwidth due to the multiple modes of a single beam, multiple cantilevers or cantilever array integrated in one energy harvesting device can provide continuous wide bandwidth if the geometric parameters of the harvester are appropriately selected.

Yang and Yang (2009) suggested using connected or coupled bimorph cantilever beams for energy harvesting, whose resonant frequencies were very close to each other and were adjustable. Figure 29 shows the schematic of the design. A theoretical analysis was conducted, and Figure 30 shows the power output versus frequency for: (1) different end mass pair with a fixed spring stiffness, and (2) different spring stiffness with a fixed mass pair ($m_0^{(1)} \neq m_0^{(2)}$). It is obvious that, with proper design of the end masses and spring, the proposed structure was able to pick up vibration energy over a wider frequency range than a single-beam harvester. The amplitude and location of the resonances were sensitive to the end spring and end masses. The drawback of the connected structure was

the reduced peak power with unequal end masses as compared with the structure with equal end masses (i.e., decoupled beams). However, unequal end masses in such connected structure are indispensable for the wider bandwidth purpose.

Using quasi-uncoupled cantilevers seems to be another option that ensures wide bandwidth but with no sacrifice of peak performance of the harvester. Since each cantilever is regarded as one substructure of the harvester, the first mode of each cantilever is one of the vibration modes of the harvester. Shahruz (2006a, 2006b) designed such an energy harvester, which comprised piezoelectric cantilevers with various lengths and tip masses attached to a common base. It was capable of resonating at various frequencies without the need of adjustment. Each cantilever had a unique resonant frequency, the combination of which into a single device created a so-called 'mechanical band-pass filter' (Figure 31(a)). By properly selecting the length and tip mass of each beam, the entire device could be designed to provide voltage response over a wider frequency range (Figure 31(b)).

Xue et al. (2008) presented another design of broadband energy harvester using multiple piezoelectric bimorphs (PB) with different thickness of piezoelectric layers and hence different operating frequency. Figure 32 shows the schematic of the design. For the multiple PBs in series, it was found that not only the power magnitude was increased but also the bandwidth (output power > 10μW) was widened from (97, 103) Hz to (87, 115) Hz, as shown in Figure 33. It was also found that the bandwidth could be shifted to the dominant frequency range by changing the number of PBs in parallel. Numerical results

showed that the bandwidth could be tailored by choosing an appropriate connection pattern (mixed series and parallel connections).

Ferrari et al. (2008) developed a multi-frequency piezoelectric converter, which has a similar schematic as Figure 31(a). It comprised three piezoelectric bimorph cantilevers with the same dimensions of 15mm×1.5mm×0.6mm but with different tip masses (m_1=1.4g, m_2=0.7g, m_3=0.6g). When excited by mechanical vibrations, the device charged the storage capacitor and when the voltage across it reached the upper and lower threshold, the circuit would connect and disconnect to deliver the energy to power a wireless sensor that transmitted the measurement. The switching time, i.e., the time interval between two measure-and-transmit operations, of a single active cantilever and combined cantilevers under different excitation frequencies are summarized in Table 3. It was observed that under resonant excitation, i.e. at either f_1, f_2, or f_3, the corresponding single cantilever in the array could alone trigger the transmission, but a single cantilever could not do so at off-resonance frequency f_4. Conversely, with the complete converter array, the converted energy was high enough to trigger the transmission for all the tested frequency, including f_4. Besides, the shorter switching time was obtained using the converter array rather than a single cantilever. It was expected that the wider bandwidth and improved performance were worth the modest increase in size of the proposed array device.

Broadband energy harvesters with cantilever array are also implemented compatibly with current standard MEMS fabrication techniques (Liu et al., 2008; Malkin and Davis, 2005;

Sari et al., 2008). Liu et al. (2008) implemented such a MEMS-based broadband energy harvester as shown in Figure 34. The AC output of three cantilevers in an array and their direct serial connection are shown in Figure 35. The phase difference was observed, which impaired the electrical accumulation of three cantilevers. The DC voltage across the capacitor after rectification was only 2.51V, and the maximum DC power output was about 3.15mW. To solve this problem, one rectifier was attached to each cantilever, as shown in Figure 36. The total DC voltage was increased to 3.93V and the maximum DC power output was about 3.98μW, though the rectification circuit consumed more electrical energy. With the wider bandwidth 226~234Hz of the prototype and the improved output from the generator array, such device was claimed to be promising in applications of ultra-low-power wireless sensor networks.

Sari et al. (2008) implemented a micro broadband energy harvester through electromagnetic induction. The reported device generated power via the relative motion between a magnet and coils fabricated on serially connected cantilevers with different lengths. It was reported that 0.4μW continuous power with 10mV voltage was generated, covering a wide external vibration frequency range of 4.2~5kHz. The test was carried out at an acceleration level of 50g, which was much higher than 0.5g in the test of Liu et al. (2008). The cantilever size had a very similar scale with that of Liu et al. (2008). However, the power output from the device by Sari et al. (2008) was much less than the device by Liu et al. (2008), which indicated that the piezoelectric conversion was more favorable for vibration energy harvesting in the MEMS scale. Furthermore, the voltage level of 10mV from the harvester in Sari et al. (2008) was impossible for AC-DC

rectification and energy storage.

3.3 Summary of multimodal energy harvesting

Multimodal energy harvesting can be implemented with a single beam by exploiting efficient energy conversion schemes in multiple modes, or with cantilever array integrated in one device (the first mode of each cantilever is one of the vibration modes of the device). Compared with the resonance tuning techniques, multimodal energy harvesting does not require any tuning efforts and hence is much easier to implement. The concerns for multimodal energy harvesting include:

(1) *Bandwidth.* In the hybrid energy harvesting scheme, the multiple effective bandwidth is quite discrete; while by using cantilever array, the targeted bandwidth can be covered continuously by proper selection of the system parameters (see Figure 33). This makes the cantilever array configuration more favorable in practice.

(2) *Energy density.* Multimodal energy harvesting increases the bandwidth accompanied by the increased volume or weight of the device, but reduces the energy density (energy/volume or energy/weight). For the cantilever array, only one cantilever or a subset of the array is active and effective for energy generating while the other cantilevers are at off-resonance status. Hence, with the known dominant spectrum of the ambient vibration, the harvester should be carefully designed with proper number and dimensions of the cantilevers such that the device can cover the targeted bandwidth with least sacrifice of energy density.

(3) *Complex circuit.* Multimodal energy harvesting requires more complex circuit than

the single conversion mechanism or single cantilever configuration. In the hybrid energy harvesting scheme, drastic difference in the magnitude of matching load for the electromagnetic and the piezoelectric case presents difficulty in combining the output power from the two mechanisms (Tadesse et al., 2009). In the cantilever array configuration, each cantilever requires one rectifier to avoid output cancellation due to the phase difference between the cantilevers (Liu et al., 2008).

4 FREQUENCY UP-CONVERSION

In many practical cases, the ambient vibration occurs at low frequency such as those caused by wind or human motions; while the resonance of a micro energy harvester may possess high resonance frequency. Hence, another frequency-robust solution for vibration energy harvesting is to amplify the source vibration frequency so that useful power can be harnessed in low frequency excitation scenarios.

4.1 Frequency up-conversion examples

One idea for frequency up-conversion is to use a mechanical gear, which can be found in the design of a windmill by Priya (2005), as shown in Figure 37. For a given rotation speed n of the windmill and m pieces of piezoelectric bimorph blades and stoppers, each blade can go through ($m \times n$) Hz oscillation.

Actually, in the piezoelectric windmill design, another frequency up-conversion mechanism was included, which was presented as the concept of two-stage energy

harvesting design by Rastegar et al. (2006) or similarly termed as a "mechanical rectification approach" by Tieck et al. (2006). The basic operation of such a two-stage energy harvester is shown in Figure 38. When the tooth passes and impacts on the cantilever tip, the cantilever will be excited and then freely vibrates at its natural frequency. Thus, the low-frequency vibration of the primary vibrating unit (i.e. the mass) can be transferred to high frequency vibrations of the secondary vibration units (i.e. the piezoelectric cantilevers), hence providing one frequency-robust vibration energy harvesting solution in low-frequency excitation scenarios. The primary challenge in such a design is the method to avoid mechanical loss such as that from impact. This frequency up-conversion technique was further pursued in the generator for low and variable speed rotary machinery (Figure 39), the ocean wave energy harvester for buoys (Figure 40) and the broadband energy harvester by Wickenheiser and Garcia (2010). Pairs of magnets or ferromagnetic structures were used to induce impulses to the beam and hence transfer the mechanical energy without contacting the elements, thus avoiding any loss caused by impact.

The frequency up-conversion technique can be more significant in the design of micro-scale energy harvesting devices, in which the resonance frequency of the structure can be at the level of 1kHz, while the ambient vibration frequency is generally below 100Hz. One novel micro vibration energy harvester using frequency up-conversion was developed by Lee et al. (2007). As shown in Figure 41, it consists of a sharp probe, micro ridges, a micro slider and a piezoelectric bimorph cantilever. The micro ridges were attached onto a micro slider mechanism. A probe tip attached on the edge of a

piezoelectric cantilever traveled along the ridges to vibrate the cantilever. In their experiment, such device could generate 225μW/cm^2 with 7 rectifications at 60Hz input frequency, which was substantially larger than the conventional resonance approaches.

Kulah and Najafi (2008) presented another design of micro electromagnetic generator using frequency up-conversion. Figure 42 shows the schematic of their proposed generator. The top permanent magnet shown in Figure 42(a) serves as the lower resonator, which can be easily deflected in the 1~100Hz range due to its large size and soft spring. The bottom resonator is a cantilever beam (or array of beams) with a higher resonance frequency. A magnetic tip on the beam could be attracted by the top magnet to excite the beam. A coil attached on the beam and the bottom permanent magnet provided the electromagnetic current induction. As the top magnet resonated in response to external low-frequency vibration, the cantilever could be caught or released at certain points, thus resonating at its high natural frequency (1~20kHz).

The proposed system was designed and tested in macro scale (Figure 43(a)). Figure 43(b) shows the measured voltage output of the prototype. The device generated a maximum instantaneous power and voltage of 120nW and 6mV at 64Hz, respectively. For micro scale implementation, it was expected that a maximum instantaneous power of 3.97μW could be generated from a single cantilever vibrating at 25Hz in vacuum. Within the overall generator area of 4mm^2, using series-connected cantilevers could further increase the power level. For the same ambient vibration frequency, the generated power by using such up-conversion technique was claimed to be more than two orders larger than a

conventional large mass/coil system.

4.2 Summary of frequency up-conversion

Frequency up-conversion can be implemented by using a mechanical gear and by a two-stage design. By using a gear (Priya, 2005; Rastegar and Murray, 2009), the input frequency can be amplified according to the number of gear teeth. In the two-stage design, the low excitation frequency can be further amplified to the high natural frequency of the cantilever beam (Rastegar et al., 2006; Lee et al., 2007; Tieck et al., 2006; Wickenheiser and Garcia, 2010; Kulah and Najafi, 2008). Such techniques decouple the excitation frequency and the vibration frequency of an energy harvester (i.e., its resonance frequency). Hence, their energy harvesting performances are insensitive to the excitation frequency as long as it is less than the resonance frequency of the harvester. These techniques are advantageous over the zigzag structure for energy harvesting at low excitation frequency (Karami and Inman, 2009) where limited bandwidth remains. They are also favorable in energy harvesting using MEMS device under low-frequency excitations, in which the resonance tuning or multimodal energy harvesting techniques do not work due to the drastic difference between the low excitation frequency and the high MEMS resonance frequency.

5 NONLINEAR TECHNIQUES FOR WIDER BANDWIDTH

Section 2 presents several techniques using magnets (Challa et al., 2008; Reissman et al., 2009; Zhu et al., 2008), which actually generate a nonlinear stiffness, to tune the

resonance of the system such that the energy harvester could be more frequency-robust in frequency variable situations. However, rather than resonance tuning, the nonlinearity of the system itself can improve the performance of the energy harvester over a wider bandwidth. As reported in the available literature, the nonlinearities of energy harvesters are considered from two perspectives, i.e., nonlinear stiffness (Ramlan et al., 2010; Mann and Sims, 2009; Stanton et al., 2009; Erturk et al., 2009; Marinkovic and Koser, 2009; Soliman et al., 2009; Lin et al., 2010; Stanton et al., 2010) and nonlinear piezoelectric coupling (Triplett and Quinn, 2009). Compared to the nonlinear piezoelectric coupling, which results from the manufacturing process of piezoelectric material, the nonlinear stiffness of a harvester is relatively easier to achieve and control. Hence in this section, recent advances in designing systems with nonlinear stiffness and their benefits for broadband energy harvesting performance are reviewed.

The dynamics of a general oscillator can be described as

$$\ddot{x} = -\frac{dU(x)}{dx} - \gamma\dot{x} + f(t) \tag{4}$$

where x represents the position of the oscillator; γ represents the viscous friction coefficient; $f(t)$ is the force input by the ambient vibration; and $U(x)$ is the potential function. If an electromagnetic generator is considered, then γ also includes the viscous damping caused by electromagnetic coupling. For a piezoelectric generator, the damping caused by piezoelectricity cannot be modeled as a viscous damper (Erturk and Inman, 2008b) and Eqn. (4) should be modified by adding a coupling term as

$$\ddot{x} = -\frac{dU(x)}{dx} - \gamma\dot{x} + \kappa V + f(t) \tag{5}$$

where κ represents the electromechanical coupling coefficient and V is the voltage on the electrical load. The circuit equations for the piezoelectric and the electromagnetic harvesters are quite different due to differences in their internal impedances. They are not given here as they can be readily found in the literature related to piezoelectric and electromagnetic conversion, such as Erturk et al. (2009) and El-Hami et al. (2001). Usually, the potential energy function $U(x)$ can be considered in a quadratic form as (Cottone et al., 2009; Gammaitoni et al., 2009):

$$U(x) = -\frac{1}{2}ax^2 + \frac{1}{4}bx^4 \tag{6}$$

The potential function $U(x)$ is symmetric and bistable for $a > 0$, and monostable for $a \le 0$. In the bistable case, two minima at $x_m = \pm\sqrt{a/b}$ are separated by a barrier at $x = 0$. For both monostable and bistable cases, the benefits on improving the bandwidth of the vibration energy harvester are discussed in the following sections.

5.1 Monostable nonlinear energy harvesters

Substituting Eqn. (6) into (4), we can obtain the forced Duffing's equation, which is widely used in modeling nonlinear energy harvester (Ramlan et al., 2010; Mann and Sims, 2009; Moehlis et al., 2009),

$$\ddot{x} + \gamma\dot{x} - ax + bx^3 = f(t) \tag{7}$$

For $a \le 0$, it can be used to describe a monostable system. $b > 0$ determines a hardening system response, while $b < 0$ a softening response.

Ramlan et al. (2010) investigated the hardening mechanism of the nonlinear monostable

energy harvester. By numerical and analytical studies, it was found that ideally, the maximum amount of power harvested by a system with a hardening stiffness was the same as the maximum power harvested by a linear system, irrespective of the degree of nonlinearity. However, this might occur at a different frequency depending on the degree of nonlinearity, as shown in Figure 44. Such a device has a larger bandwidth over which the significant power can be harvested due to the shift in the resonance frequency.

Mann and Sims (2009) presented a design for electromagnetic energy harvesting from the nonlinear oscillations of magnetic levitation. Figure 45 shows the schematic of the system where two outer magnets are oriented to repel the center magnet, thus suspending it with a nonlinear restoring force. The derived governing equation has the same form as Eqn. (7). Figure 46 shows the experimental velocity response and theoretical predictions under low and high harmonic base excitation levels, respectively. At low excitation level, the frequency response (Figure 46(a)) was similar to the response of a linear system. However, at high excitation level, the response curve was bent to the right (Figure 46(b)). Thus, relatively large amplitudes persisted over a much wider frequency range. However, such a device using hardening mechanism can only broaden the frequency response in one direction (the peak response shifts to the right).

Stanton et al. (2009) proposed another monostable nonlinear device for energy harvesting through piezoelectric effect. The device consists of a piezoelectric beam with a magnetic end mass interacting with the field of oppositely poled stationary magnets, as shown in Figure 47. The system was modeled by an electromechanically coupled Duffing's

equation similar to Eqn. (7), except that the piezoelectric coupling term κV should be added as we did in Eqn. (5). By tuning the nonlinear magnetic interactions around the end mass (i.e. tuning the distance *d*), both hardening and softening responses may occur, as shown in Figure 48, which allows the frequency response to be broadened bi-directionally. In the experimental validation, a linearly decreasing frequency sweep was performed for the softening case. The energy harvesting performance of the nonlinear configuration and the linear configuration (i.e. with two stationary magnets removed) was compared, as shown in Figure 49. The results showed that not only a wider bandwidth but also a better performance could be obtained by the nonlinear energy harvester, as compared to the linear configuration. The advantage imparted in the nonlinearity depends on realizing the high-energy attractor (Stanton et al., 2009). A linearly decreasing or increasing frequency sweep can capture the high-energy attractor, and hence improve the output power and bandwidth for the softening and hardening cases, respectively. Unfortunately, such conditions cannot be guaranteed in practice. A momentary perturbation would be required if low-energy branch manifests, but the requisite actuation energy was not addressed in their work.

Obviously, the wider bandwidth achieved in Ramlan et al. (2010), Mann and Sims (2009) and Stanton et al. (2009) and the performance comparison results between the linear and the monostable nonlinear devices are conditionally validated. If the nonlinear devices cannot capture and maintain the dynamics near the high-energy branch by certain means of excitation or perturbation, little power can be harnessed. Daqaq (2010) demonstrated that under White Gaussian excitation environment, the hardening-type nonlinearity failed

to provide any enhancement of output power over the typical linear harvesters. Under Colored Gaussian excitations, the expected output power even decreased with such hardening-type nonlinearity.

5.2 Bistable nonlinear energy harvester

For $a > 0$, Eqn. (7) can be used to describe a bistable nonlinear system. In this section, it is discussed in detail on how to exploit the properties of the nonlinearity of a bistable system to improve energy harvesting performance over a wide range of ambient vibration frequencies, subjected to either periodic forcing or stochastic forcing.

5.2.1 Periodic forcing

A periodically forced oscillator can undergo various types of large-amplitude oscillations, including chaotic oscillation, large-amplitude periodic oscillation and large-amplitude quasi-periodic oscillation. The behavior depends on the design of the device, the frequency and amplitude of the forcing and the damping (Moehlis et al., 2009).

Moehlis et al. (2009) presented one example of bistable oscillator under periodic forcing with the following governing equation

$$\ddot{x} + 0.1\dot{x} - x + x^3 = \cos(\omega t) \tag{8}$$

In the bifurcation analysis of this forced Duffing's oscillator (plotting the instantaneous value of x whenever $\dot{x} = 0$ for each ω by getting rid of transients), they found that large amplitude response (x>1 and x<-1) occurred over a wide range of driving frequencies and even extended to very low frequencies.

One physically realizable energy harvester with nonlinear bistable stiffness was proposed by Ramlan et al. (2010), termed *snap-through* mechanism. The setup consisted of two linear oblique springs connected to a mass and a damper as shown in Figure 50, yielding a non-linear restoring force in the x direction. This mechanism has the effect of steepening the displacement response of the mass as a function of time, resulting in a higher velocity for a given input excitation. Numerical results revealed that this mechanism could provide much better performance than the linear mechanism when the excitation frequency was much less than the natural frequency.

Nonlinear bistable stiffness can also be created by using magnets. Erturk et al. (2009) pursued such method in designing a broadband piezomagnetoelastic generator. The device consisted of a ferromagnetic cantilevered beam with two permanent magnets located symmetrically near the free end, and subjected to harmonic base excitation. Two piezoceramic layers were attached to the root of the cantilever for energy generation, as illustrated in Figure 51. For an initial deflection at one of the stable equilibrium, the voltage response could be chaotic strange attractor motion or large-amplitude periodic motion (limit cycle oscillation), under small or large excitation amplitude, as shown in Figures 52(a) and (b). The large-amplitude periodic motion could also be obtained under small excitation level by simply applying a disturbance or equivalently an initial velocity condition, as shown in Figure 52(c). By such, the large-amplitude response could be obtained at *off-resonance* frequencies. Hence, the piezomagnetoelastic generator could produce broadband performance, advantageous over the linear piezoelastic configuration

(with two magnets removed), as shown in Figure 53. However, for small excitation amplitude, actuation energy is required to perturb the beam and hence drive the system into high-energy orbits, which was not investigated in their work.

5.2.2 Stochastic forcing

For a bistable system, stochastic forcing can also induce transitions between the stable equilibria of the system, giving large-amplitude oscillations.

Cottone et al. (2009) realized a piezoelectric inverted pendulum by using the bistable mechanism. Figure 54 shows the schematic of their experimental apparatus. The potential functions of the pendulum for different distance Δ between polar opposing magnets are shown in Figure 55. When Δ was small enough, two equilibrium positions appeared. The random vibration made the pendulum swing with small oscillations around each equilibrium and large excursions from one to another. However, for extremely small Δ, the pronounced barrier of the potential function (Figure 55) confined the pendulum swing within one potential well. For specific Δ and noise level, the position x_{rms} reached a maximum and hence the maximum power could exceed by 4~6 times of the power obtained when the magnets were far away, as shown in Figure 56. For the bistable pendulum and a more general bistable dynamical system, the x_{rms} was found governed by two main contributions: (i) the raising, mainly due to growth of the separation between the two minima of the potential function; and (ii) the drop, mainly due to decrease in the jump probability caused by the increase of the potential barrier height ΔU.

Ferrari et al. (2009) followed the idea of Cottone et al. (2009) and further studied the energy harvesting performance from wide-spectrum vibrations for a bistable piezoelectric beam by magnets with opposite poles, as shown in Figure 57. Under white-noise excitation, when the magnets approached each other, transition between the two stable states occurred and the output voltage significantly increased, as shown in Figure 58(a). From the frequency amplitude spectra of output voltage (Figure 58(b)), a wider spectrum for the bistable configuration (d=10.5mm) was observed than for the quasi-linear case (d=25.0mm).

One way to further improve the performance of a bistable system is to increase the probability of transition between the potential wells. McInnes et al. (2008) proposed to exploit the phenomenon of stochastic resonance to enhance the performance of a bistable system for energy harvesting. The stochastic resonance can occur if the dynamics of the system are forced such that the potential barrier oscillates, and this forcing is matched to the mean time between transitions — inverse Kramer's rate (Wellens et al., 2004). For a beam clamped at both ends, the one DOF bistable model is shown in Figure 59. This is similar to the *snap-through* setup by Ramlan et al. (2010), except that the distance *A-A'* can be modulated at frequency ω and hence the potential barrier is modulated. Thus the dynamics of the mechanism are parametrically forced and are defined by

$$\ddot{\xi} + c\dot{\xi} - \mu(1 - \eta\cos(\omega t))\xi + \xi^3 = Q(t) \tag{9}$$

where ξ is the non-dimensional coordinate; c is the damping coefficient; μ is a measure of the compressive load acting on the beam; η and ω are the magnitude and frequency of forcing for modulation, respectively; and $Q(t)$ is the external noise. The tuned system in

stochastic resonance by forcing (i.e. the forcing was matched to inverse Kramer's rate) apparently experienced larger amplitude vibrations than those of the unforced mechanism, which were confined in a single potential well, as shown in Figure 60. Thus, significantly more energy was obtained. However, if the system was un-tuned, the net energy generated by the forcing mechanism could be less than the unforced mechanism, considering the energy consumed for forcing the beam.

5.3 Summary of nonlinear techniques for wider bandwidth

This section concentrates on the benefits of nonlinearity of a system for energy harvesting performance over a wide bandwidth, with a focus on nonlinear stiffness. The nonlinear energy harvester, with the nonlinearity either introduced mechanically or by using magnets, usually can be designed as a monostable or bistable device.

(1) *Monostable nonlinear energy harvester.* No matter in hardening or softening configurations, with the nonlinearity engaged, the resonance curve will either be bent to the right or left. When the nonlinearity is large enough, broad bandwidth is possible to achieve. The advantage imparted in the nonlinearity depends on the implementation of high-energy attractor. A linearly decreasing or increasing frequency sweep for softening and hardening case respectively can capture the high-energy attractor motion and hence improve the output power and bandwidth. However, such characteristics limit its practical application, i.e., the monostable energy harvester can only work in the condition with slow and proper frequency sweep. Besides, since multi-value and jump phenomenon near resonance also occur

with the increased nonlinearity (Figure 46(b) and Figure 48), a mechanism should be implemented to perturb and drive the system into high amplitude motion in case the system vibrates into a low-energy branch.

(2) *Bistable nonlinear energy harvester*. For a bistable system, large-amplitude oscillation can occur under both periodic forcing and stochastic forcing. Under high level periodic forcing or low level forcing with disturbance, the bistable harvester can be driven into high-energy orbits. Hence, its performance can outperform the linear device covering a wide bandwidth. Under stochastic or noise forcing, the bistable system also shows significant performance improvement when the system parameters are properly selected, such as the distance between magnets Δ in Cottone et al. (2009). The performance of the bistable harvester can be further improved by exploiting the stochastic resonance, in which the boundary should be properly forced to periodically change the potential barrier of the system and hence the probability of the large-amplitude transition between the two stable states. However, such methods require external energy input and are more difficult to implement.

6 CONCLUSIONS

The fundamental drawback of linear resonating harvesters, i.e., the narrow bandwidth, limits their application in practical scenarios where the ambient vibration source is frequency-variable or totally random. The focus of this review paper, as summarized below, is on the current advances in broadband energy harvesting techniques, including resonance tuning techniques, multimodal energy harvesting, frequency up-conversion and

nonlinear techniques.

- *Resonance tuning techniques.* Generally, the mechanical and magnetic tuning methods can achieve larger tunability as compared with the piezoelectric tuning methods. However, most of them are difficult to implement during operation and the system parameters should be adjusted manually. For the magnetic methods, one more drawback is that the system may require further power to perturb it into high amplitude branch vibration, due to the nonlinearity caused by using the magnets, similar to what exists in the nonlinear techniques described in Section 5. Resonance tuning by piezoelectric transducers is easier to implement by applying voltage to the actuators or operating the control circuit to vary the shunt damping load. Thus, the device can be designed for automatic tuning during operation. However, the tunability by piezoelectric methods is more limited. Another weakness is that the power required for tuning in most related devices outweighs the power harvested in the active tuning mode except that of Wu et al. (2006). All the methods can be further categorized into active and passive tuning. With affordable low power required for tuning, active tuning can work under excitation with fast-varying frequency or random excitation, while passive tuning can only work under excitation with slow-varying frequency.
- *Multimodal energy harvesting.* Multimodal energy harvesting does not require any tuning efforts and hence is much easier to implement. It can be implemented with a single beam by exploiting efficient energy conversion schemes in multiple modes or with cantilever array integrated in one device (the first mode of each cantilever is

regarded as one of the vibration modes of the entire device). The former provides a discrete bandwidth while the latter can be exploited to cover continuous bandwidth, which makes the latter more favorable in practice. However, the cantilever array device should be carefully designed with the proper number and dimensions of the cantilevers so that it can cover the targeted bandwidth with least sacrifice of the energy density. Additionally, in both techniques, a more complex energy storage circuit is required.

- *Frequency up-conversion*. In low excitation scenarios, the input excitation frequency can be amplified by using a mechanical gear, or by the two-stage design in which the low excitation frequency can be amplified to the high natural frequency of the cantilever beam. Such techniques are favorable in energy harvesting for MEMS devices where the resonance tuning or multimodal energy harvesting techniques do not work due to the drastic difference between the low excitation frequency and the high MEMS resonance frequency.
- *Nonlinear techniques.* Nonlinearities can also be exploited to improve the system performance over wider bandwidth. For the monostable nonlinear system, the dynamics near the high-energy branch can be maintained by slow and proper frequency sweep such that the output power and bandwidth can be improved. However, such condition cannot be guaranteed in practice. Additionally, Daqaq (2010) demonstrated that under random excitation, a hardening-type monostable harvester was unable to provide better performance over a linear harvester. The bistable nonlinear system can conditionally achieve improved energy harvesting performance under both periodic and stochastic forcing. Hence, the bistable system

is more applicable in practice since the ambient vibrations are pervasively stochastic. Its performance can be further improved by exploiting the stochastic resonance. However, both monostable and bistable systems may require certain mechanism to disturb and drive them into motion in the high-energy branch under periodic forcing. How to design such mechanism for perturbation and to implement the condition for stochastic resonance with lowest power may be the future directions of research for these nonlinear techniques.

Obviously, there are some other broadband techniques which cannot be categorized into the four groups described in this review paper, for example, the technique on employing an optimal inductor (Renno et al., 2009). Additionally, each technique reviewed in this paper is only preferable in some specific conditions. A suitable technique for broadband vibration energy harvesting should be selected according to whether the excitation is periodic or stochastic, whether the excitation frequency varies infrequently, and what the excitation level and targeted frequency range are, etc. The merits, weakness and applicability of current techniques are summarized in Table 4. The authors hope that it can provide some guidance to the researchers when they want to develop a vibration-based energy harvester. It is envisioned that, with further improvement of these broadband techniques, the concept of energy harvesting is approaching practical deployment in the industrial applications as well as in our daily life.

ACKNOWLEDGEMENT

The authors sincerely thank the editor and reviewers for their insightful review and

invaluable suggestions, making this a better paper.

REFERENCES

Anton, S.R. and Sodano, H.A. 2007. "A Review of Power Harvesting Using Piezoelectric Materials (2003-2006)," *Smart Mater. Struct.*, 16:R1-R21.

Challa, V.R., Prasad, M.G. and Fisher, F.T. 2009. "A Coupled Piezoelectric-Electromagnetic Energy Harvesting Technique for Achieving Increased Power Output through Damping Matching," *Smart Mater. Struct.*, 18:095029.

Challa, V.R., Prasad, M.G., Shi, Y. and Fisher, F.T. 2008. "A Vibration Energy Harvesting Device with Bidirectional Resonance Frequency Tunability," *Smart Mater. Struct.*, 17:015035.

Cottone, F., Vocca, H. and Gammaitoni, L. 2009. "Nonlinear Energy Harvesting." *Phys. Rev. Lett.*, 102: 080601.

Daqaq, M.F. 2010. "Response of Uni-Modal Duffing-Type Harvesters to Random Forced Excitations," *J. Sound Vib.*, 329:3621–3631.

De Marqui, Jr. C., Erturk, A. and Inman, D.J. 2009. "An Electromechanical Finite Element Model for Piezoelectric Energy Harvester Plates," *J. Sound Vib.*, 327:9-25.

Eichhorn, C., Goldschmidtboeing, F. and Woias, P. 2008. "A Frequency Tunable Piezoelectric Energy Converter Based on A Cantilever Beam," *Proceedings of PowerMEMS*, 309-312.

El-Hami, M., Glynne-Jones, P., White, N.M., Beeby, S., James, E., Brown, A.D. and Ross, J.N. 2001. "Design and Fabrication of A New Vibration-Based Electromechanical Power Generator," *Sens. Actuat. A*, 92:335-342.

Erturk, A., Hoffmann, J. and Inman, D.J. 2009. "A Piezomagnetoelastic Structure for Broadband Vibration Energy Harvesting," *Appl. Phys. Lett.*, 94:254102.

Erturk, A. and Inman, D.J. 2008a. "A Distributed Parameter Electromechanical Model for Cantilevered Piezoelectric Energy Harvesters," *J. Vib. Acoust.*, 130:041002.

Erturk, A. and Inman, D.J. 2008b. "Issues in Mathematical Modeling of Piezoelectric Energy Harvesters," *Smart Mater. Struct.*, 17:065016.

Ferrari, M., Ferrari, V., Guizzetti, M., Andò, B., Baglio, S. and Trigona, C. 2009. "Improved Energy Harvesting from Wideband Vibrations by Nonlinear Piezoelectric Converters," *Procedia Chemistry*, 1:1203-1206.

Ferrari M., Ferrari, V., Guizzetti, M., Marioli, D. and Taroni, A. 2008. "Piezoelectric Multifrequency Energy Converter for Power Harvesting in Autonomous Microsystems," *Sens. Actuat. A*, 142:329-335.

Gammaitoni, L., Neri, I. and Vocca, H. 2009. "Nonlinear Oscillators for Vibration Energy Harvesting," *Appl. Phys. Lett.*, 94:164102.

Hu, Y., Xue, H. and Hu, H. 2007. "A Piezoelectric Power Harvester with Adjustable Frequency through Axial Preloads," *Smart Mater. Struct.*, 16:1961-1966.

Karami, M.A. and Inman, D.J. 2009. "Vibration Analysis of the Zigzag Micro-Structure for Energy Harvesting," *Proceedings of SPIE*, 7288:728809.

Kulah, H. and Najafi, K. 2008. "Energy Scavenging from Low-Frequency Vibrations by Using Frequency Up-Conversion for Wireless Sensor Applications," *IEEE Sensors Journal*, 8:261-268.

Lee, D., Carman, G., Murphy, D. and Schulenburg, C. 2007. "Novel Micro Vibration Energy Harvesting Device Using Frequency Up Conversion," *Proceedings of 14th*

International Conference on Solid-State Sensors, Actuators and Microsystems, 871-874.

Leland, E.S. and Wright, P.K. 2006. "Resonance Tuning of Piezoelectric Vibration Energy Scavenging Generators Using Compressive Axial Preload," *Smart Mater. Struct.*, 15:1413-1420.

Lin, J., Lee, B. and Alphenaar, B. 2010. "The Magnetic Coupling of A Piezoelectric Cantilever for Enhanced Energy Harvesting Efficiency," *Smart Mater. Struct.*, 19:045012.

Liu, J., Fang, H., Xu, Z., Mao, X., Shen, X., Chen, D., Liao, H. and Cai, B. 2008. "A MEMS-Based Piezoelectric Power Generator Array for Vibration Energy Harvesting," *Microelectronics Journal*, 39:802-806.

Loverich, J., Geiger, R. and Frank, J. 2008. "Stiffness Nonlinearity as A Means for Resonance Frequency Tuning and Enhancing Mechanical Robustness of Vibration Power Harvesters," *Proceedings of SPIE*, 6928:692805.

MacCurdy, R.B., Reissman, T. and Garcia, E. 2008. "Energy Management of Multi-Component Power Harvesting Systems," *Proceedings of SPIE*, 6928:692809.

Malkin, M.C. and Davis, C.L. 2005. "Multi-frequency Piezoelectric Energy Harvester," *US Patent 6858970 B2*.

Mann, B.P. and Sims, N.D. 2009. "Energy Harvesting from The Nonlinear Oscillations of Magnetic Levitation," *J. Sound Vib.*, 319:515-530.

Marinkovic, B. and Koser, H. 2009. "Smart Sand — A Wide Bandwidth Vibration Energy Harvesting Platform," *Appl. Phys. Lett.*, 94:103505.

McInnes, C.R., Gorman, D.G. and Cartmell, M.P. 2008. "Enhanced Vibrational Energy Harvesting Using Nonlinear Stochastic Resonance," *J. Sound Vib.*, 318:655-662.

Micheson, P.D., Green, T.C., Yeatman, E.M. and Holmes, A.S. 2004. "Architectures for Vibration-Driven Micropower Generators," *J. Microelectromech. Syst.*, 13:429-440.

Moehlis, J., DeMartini, B.E., Rogers, J.L. and Turner, K.L. 2009. "Exploiting Nonlinearity to Provide Broadband Energy Harvesting," *Proceedings of ASME Dynamic Systems and Control Conference*, DSCC2009-2542.

Morris, D.J., Youngsman, J.M., Anderson, M.J. and Bahr, D.F. 2008. "A Resonant Frequency Tunable, Extensional Mode Piezoelectric Vibration Harvesting Mechanism," *Smart Mater. Struct.*, 17:065021.

Murray, R. and Rastegar, J. 2009. "Novel Two-Stage Piezoelectric-Based Ocean Wave Energy Harvesters for Moored or Unmoored Buoys," *Proceedings of SPIE*, 7288:72880E.

Paradiso, J.A. and Starner, T. 2005. "Energy Scavenging for Mobile and Wireless Electronics," *IEEE Pervasive Computing*, 4:18-27.

Peters, C., Maurath, D., Schock, W., Mezger, F. and Manoli, Y. 2009. "A Closed-Loop Wide-Range Tunable Mechanical Resonator for Energy Harvesting Systems," *J. Micromech. Microeng.*, 19:094004.

Priya, S. 2005. "Modeling of Electric Energy Harvesting Using Piezoelectric Windmill," *Appl. Phys. Lett.*, 87:184101.

Ramlan, R., Brennan, M.J., Mace, B.R. and Kovacic, I. 2010. "Potential Benefits of A Non-linear Stiffness in An Energy Harvesting Device," *Nonlinear Dynamics*, 59:545-558.

Rastegar, J. and Murray, R. 2009. "Novel Two-Stage Piezoelectric-Based Electrical Energy Generators for Low and Variable Speed Rotary Machinery," *Proceedings of SPIE*, 7288:72880B.

Rastegar, J., Pereira, C. and Nguyen, H-L. 2006. "Piezoelectric-Based Power Sources for Harvesting Energy from Platforms with Low-Frequency Vibration," *Proceedings of SPIE*, 6171:617101.

Reissman, T., Wolff, E.M. and Garcia, E. 2009. "Piezoelectric Resonance Shifting Using Tunable Nonlinear Stiffness," *Proceedings of SPIE*, 7288:72880G.

Renno, J.M., Daqaq, M.F. and Inman, D.J. 2009. "On the Optimal Energy Harvesting from A Vibration Source," *J. Sound Vib.*, 320:386-405.

Roundy, S., Wright, P.K. and Rabaey, J. 2003. "A Study of Low Level Vibrations as A Power Source for Wireless Sensor Nodes," *Computer Communications*, 26:1131-1144.

Roundy, S. and Zhang, Y. 2005. "Toward Self-Tuning Adaptive Vibration Based Micro-Generators," *Proceedings of SPIE*, 5649:373-384.

Sari, I., Balkan, T. and Kulah, H. 2008. "An Electromagnetic Micro Power Generator for Wideband Environmental Vibrations," *Sens. Actuat. A*, 145-146:405-413.

Shahruz, S.M. 2006a. "Design of Mechanical Band-pass Filters for Energy Scavenging," *J. Sound Vib.*, 292:987-998.

Shahruz, S.M. 2006b. "Limits of Performance of Mechanical Band-Pass Filters Used in Energy Scavenging," *J. Sound Vib.*, 293:449-461.

Soliman, M.S.M., Abdel-Rahman, E.M., El-Saadany, E.F. and Mansour, R.R. 2009. "A Design Procedure for Wideband Micropower Generators," *J. Microelectromech. Syst.*, 18:1288-1299.

Stanton, S.C., McGehee, C.C. and Mann, B.P. 2009. "Reversible Hysteresis for Broadband Magnetopiezoelastic Energy Harvesting," *Appl. Phys. Lett.*, 95:174103.

Stanton, S.C., McGehee, C.C. and Mann, B.P. 2010. "Nonlinear Dynamics for Broadband Energy Harvesting: Investigation of A Bistable Piezoelectric Inertial Generator," *Physica D*, 239:640-653.

Tadesse, Y., Zhang, S. and Priya, S. 2009. "Multimodal Energy Harvesting System: Piezoelectric and Electromagnetic," *J. Intell. Mater. Syst. Struct.*, 20:625-632.

Tieck, R.M., Carman, G.P. and Lee, D.G.E. 2006. "Electrical Energy Harvesting Using A Mechanical Rectification Approach," *Proceedings of IMECE2006*, 547-553.

Triplett, A. and Quinn, D.D. 2009. "The Effect of Non-linear Piezoelectric Coupling on Vibration-based Energy Harvesting," *J. Intell. Mater. Syst. Struct.*, 20:1959-1967.

Wellens, T., Shatokhin, V. and Buchleitner, A. 2004. "Stochastic Resonance," *Reports on Progress in Physics*, 67:45-105.

Wickenheiser, A.M. and Garcia, E. 2010. "Broadband Vibration-Based Energy Harvesting Improvement through Frequency Up-Conversion by Magnetic Excitation," *Smart Mater. Struct.*, 19:065020.

Wischke, M., Masur, M., Goldschmidtboeing, F. and Woias, P. 2010. "Electromagnetic Vibration Harvester with Piezoelectrically Tunable Resonance Frequency," *J. Micromech. Microeng.*, 20:035025.

Wu, W., Chen, Y., Lee, B., He, J. and Peng, Y. 2006. "Tunable Resonant Frequency Power Harvesting Devices," *Proceedings of SPIE*, 6169:61690A.

Wu, X., Lin, J., Kato, S., Zhang, K., Ren, T. and Liu, L. 2008. "A Frequency Adjustable Vibration Energy Harvester," *Proceedings of PowerMEMS*, 245-248.

Xue, H., Hu, Y. and Wang, Q. 2008. "Broadband Piezoelectric Energy Harvesting Devices Using Multiple Bimorphs with Different Operating Frequencies," *IEEE Transactions on Ultrasonics, Ferroelectrics, and Frequency Control*, 55:2104-2108.

Yang, Y.W., Tang, L.H. and Li, H.Y. 2009. "Vibration Energy Harvesting Using Macro-Fiber Composites," *Smart Mater. Struct.*, 18:115025.

Yang, Y.W and Tang, L.H. 2009. "Equivalent Circuit Modeling of Piezoelectric Energy Harvesters," *J. Intell. Mater. Syst. Struct.*, 20:2223-2235.

Yang, Z. and Yang, J. 2009. "Connected Vibrating Piezoelectric Bimorph Beams as a Wide-band Piezoelectric Power Harvester," *J. Intell. Mater. Syst. Struct.*, 20:569-574.

Youngsman, J.M., Luedeman, T., Morris, D.J. and Andersonb, M.J. 2010. "A Model for An Extensional Mode Resonator Used as A Frequency-Adjustable Vibration Energy Harvester," *J. Sound Vib.*, 329:277-288.

Zhu, D., Roberts, S., Tudor, J. and Beeby, S. 2008. "Closed Loop Frequency Tunning of A Vibration-Based Microgenerator," *Proceedings of PowerMEMS*, 229-232.

Table 1 Ambient vibration sources (Roundy et al., 2003, copyright: Elsevier)

Vibration Sources	Acceleration (m/s^2)	Peak frequency (Hz)
Car engine	12	200
Base of 3-axis machine tool	10	70
Blender casing	6.4	121
Clothes dryer	3.5	121
Car instrument panel	3	13
Door frame just after door closes	3	125
Small microwave oven	2.5	121
HVAC vents in office building	0.2-1.5	60
Windows next to busy road	0.7	100
CD on notebook computer	0.6	75
Second storey floor of busy office	0.2	100

Table 2 Summary of the reported resonance tuning methods

Author	Methods	Tuning range	Tunability $\left(\frac{\text{frequency change}}{\text{average frequency}}\right)$	Tuning load (force, distance, voltage)	Energy or power for tuning	Automatic controller
Leland and Wright	Mechanical (passive)	200~250Hz (7.1g tip mass)	22.22%	Up to 65N	—	×
Eichhorn et al.	Mechanical (passive)	292~380Hz	26.19%	Up to 22.75N	—	×
Hu et al.	Mechanical (passive)	58.1~169.4Hz	97.85%	-50~50N	—	×
Morris et al.	Mechanical (passive)	80~235Hz (can be wider)	≧98.41%	≈1.25mm	—	×
Loverich et al.	Mechanical (passive)	56~62Hz	10.17%	0.5mm	—	×
Wu et al.	Mechanical (passive)	130~180Hz	32.26%	21mm	—	×
Challa et al.	Magnetic (passive)	22~32Hz	37.04%	3cm	85mJ	×
Reissman et al.	Magnetic (passive)	88~99.38Hz	12.15%	1.5cm	—	×
Zhu et al.	Magnetic (passive)	67.6~98Hz	36.71%	3.8mm	$2.04mJ \cdot mm^{-1}$	√
Wu et al.	Piezoelectric (active)	91.5~94.5Hz	3.23%	—	μW level (for controller)	√
Peters et al.	Piezoelectric (active)	66~89Hz (actuator PL140)	29.68%	±5V	150mW (discrete control circuit)	√
Roundy and Zhang	Piezoelectric (active)	64.5~67Hz	3.80%	5V	440μW	×
Wischke et al.	Piezoelectric (semi-passive)	20Hz (10mm long electrode)	≈6.7%	-65~+130V	200μJ	×

Table 3 Switching times with different frequency-cantilever pairs (Ferrari et al., 2008, copyright: Elsevier)

	Cantilever 1	Cantilever 2	Cantilever 3	All
f_1 = 113Hz	17.8s	×	×	14s
f_2 = 183Hz	×	25.8s	×	14.3s
f_3 = 281Hz	×	×	12.2s	6.6s
f_4 = 145Hz	×	×	×	21s

Table 4 Merits, weakness and applicability of various broadband energy harvesting techniques

Methods		Merits, weakness, and applicability
Resonance frequency tuning	Active tuning	• Mostly by piezoelectric methods. • Limited tunability. • Cost of tuning mostly outweighs the power harvested. • Continuously achievable during operation by automatic controller. • Applicable for excitation with fast-varying frequency or random excitation, given affordable power consumption for tuning.
	Passive tuning	• Mostly by mechanical and magnetic methods. • Difficult to achieve automatically and during operation. • Magnetic methods require power to perturb the harvester into high amplitude branch. • Relatively large tunability. • Applicable for excitation with slow-varying frequency.
Multimodal energy harvesting		• Much easier to implement than resonance tuning techniques. • Should be designed with proper parameters to cover the targeted frequency range with the least sacrifice of energy density. • Require complex energy storage circuit.
Frequency up-conversion		• Preferable if drastic difference exists between low excitation frequency and high natural frequency of the harvester, e.g., MEMS harvester.
Nonlinear techniques	Monostable	• Applicable for excitations with slow and proper frequency sweep. • Require perturbation if the harvester enters low-energy branch.
	Bistable	• Applicable for high-level periodic excitation. • Applicable for low-level periodic excitation but with perturbation mechanism to drive the harvester into high-energy branch. • Applicable for stochastic excitation and can further improve the performance by proper periodic change of potential barrier (stochastic resonance).

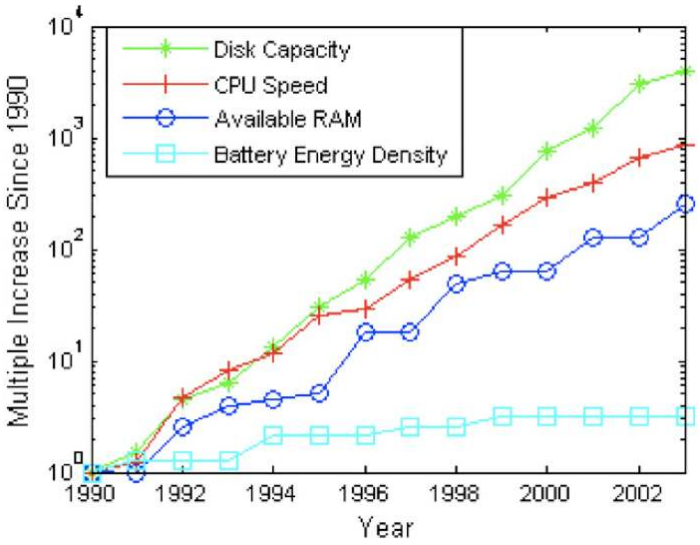

Figure 1 Trends of battery and other computing hardware technologies since 1990 (Anton and Sodano, 2007, copyright: IOP Publishing)

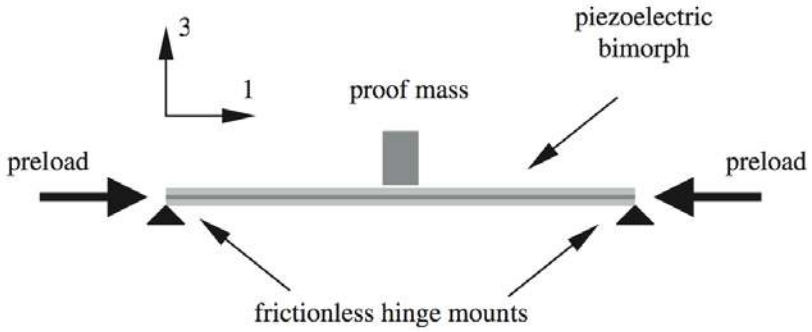

Figure 2 Schematic of a simply supported bimorph energy harvester (Leland and Wright, 2006, copyright: IOP Publishing)

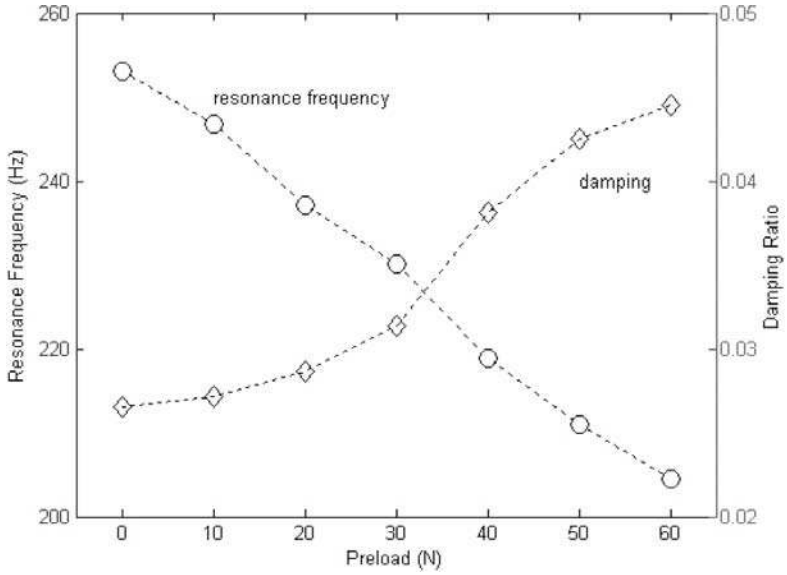

Figure 3 Resonance frequency and damping versus compressive preload (Leland and Wright, 2006, copyright: IOP Publishing)

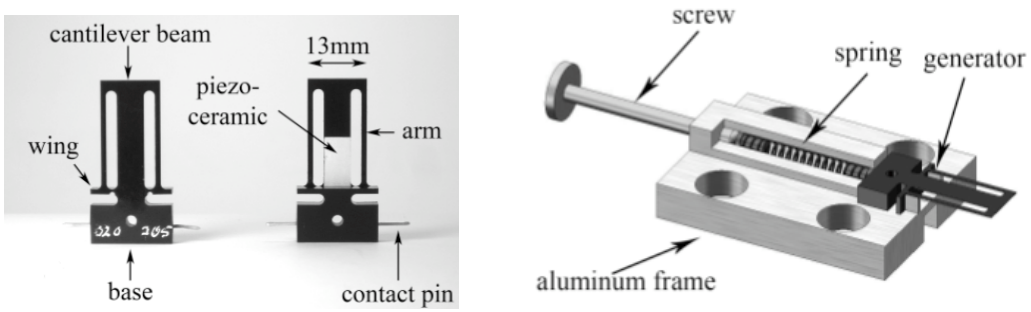

(a) (b)

Figure 4 (a) Generator with arms (upper and bottom sides); (b) Schematic of the entire setup (Eichhorn et al., 2008)

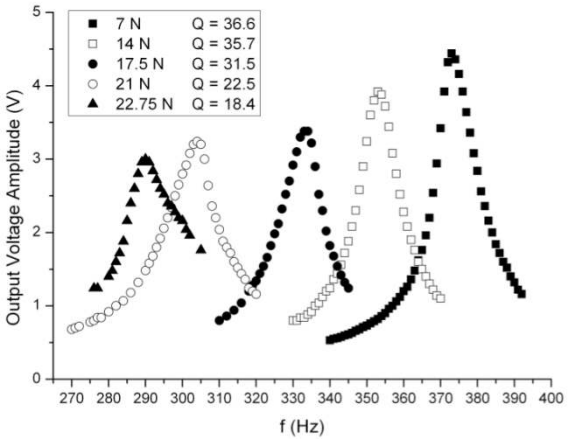

Figure 5 Resonance curves with various pre-stresses (Eichhorn et al., 2008)

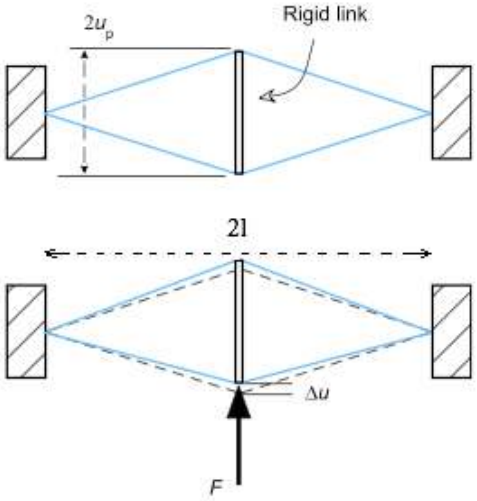

Figure 6 Pre-tensioning two membranes by a rigid link (Morris et al., 2008, copyright: IOP Publishing)

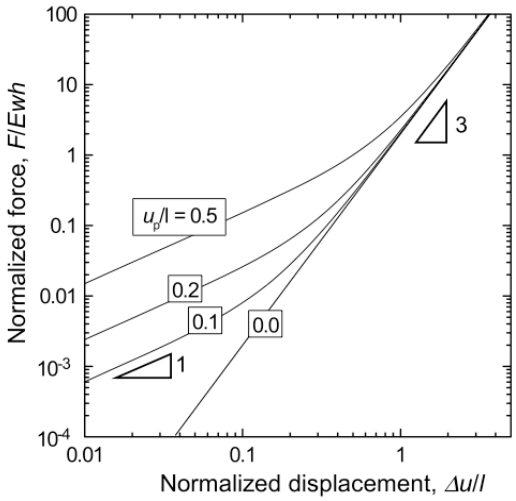

Figure 7 Normalized force–displacement relationship for an XMR with rectangular membrane (Morris et al., 2008, copyright: IOP Publishing)

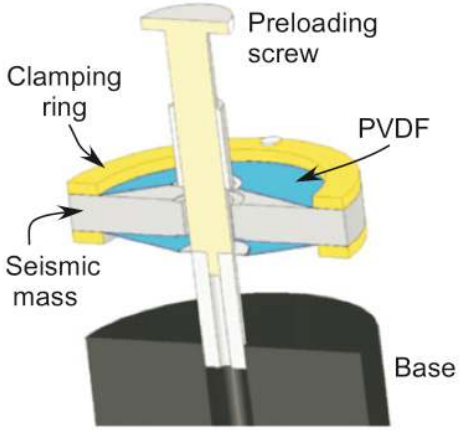

Figure 8 Cross-sectional drawing of an assembled XMR prototype (Morris et al., 2008, copyright: IOP Publishing)

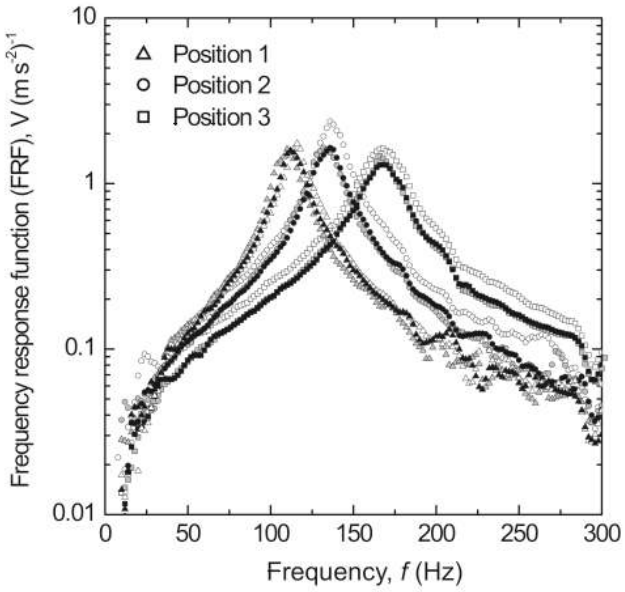

Figure 9 Frequency response functions for three adjustment positions (Morris et al., 2008, copyright: IOP Publishing)

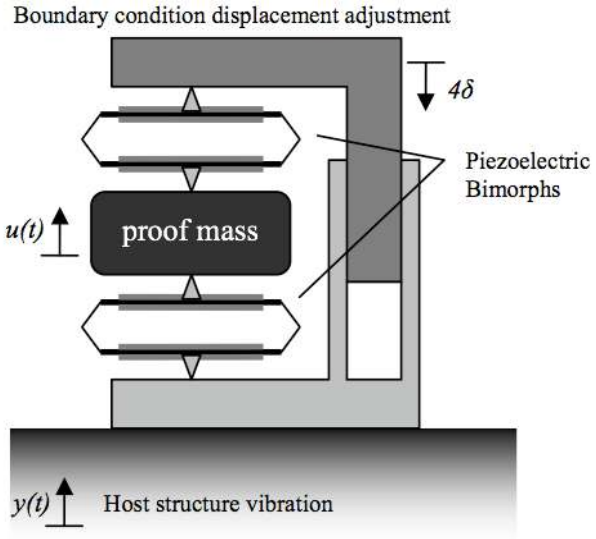

Figure 10 Energy harvester configuration with adjustable boundary condition for inducing large deformation in bimorph plates (Loverich et al., 2008, copyright: SPIE)

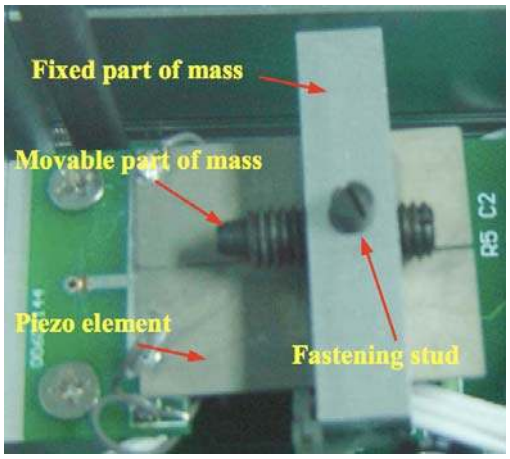

Figure 11 A piezoelectric cantilever Prototype with a moveable mass (Wu et al., 2008)

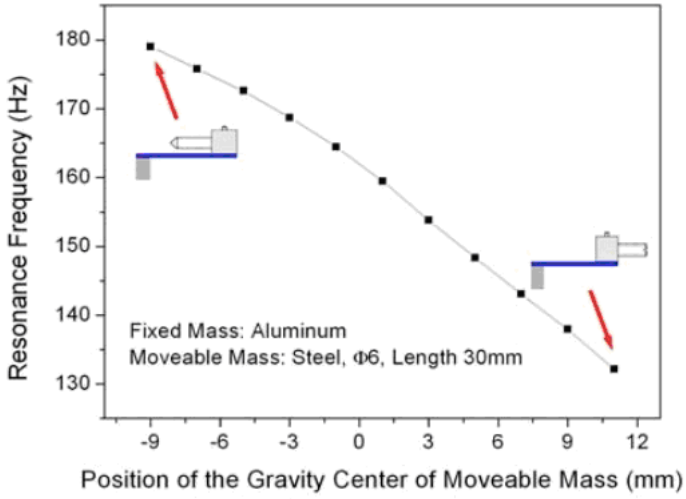

Figure 12 Resonance frequency versus the position of the gravity center of moveable mass (Wu et al., 2008)

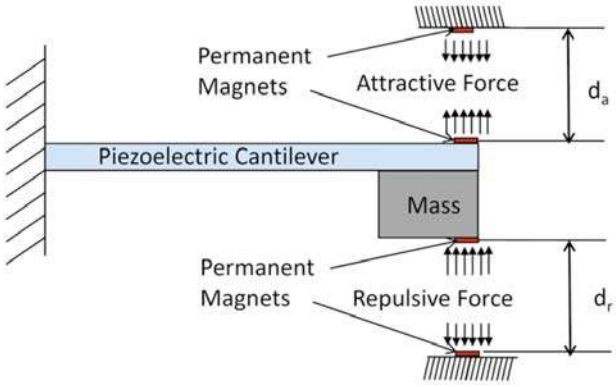

Figure 13 Schematic of the resonance tunable harvester (Challa et al., 2008, copyright: IOP Publishing)

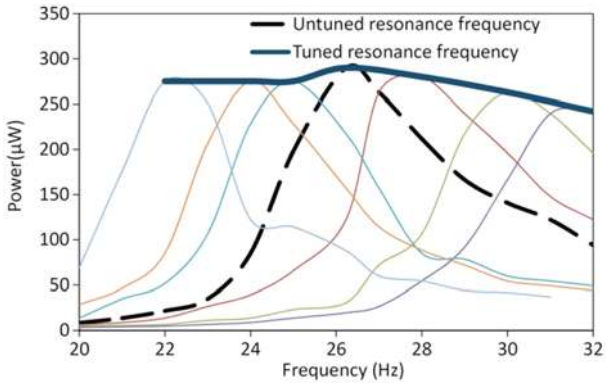

Figure 14 Experimental power output versus tuned resonance frequency (Challa et al., 2008, copyright: IOP Publishing)

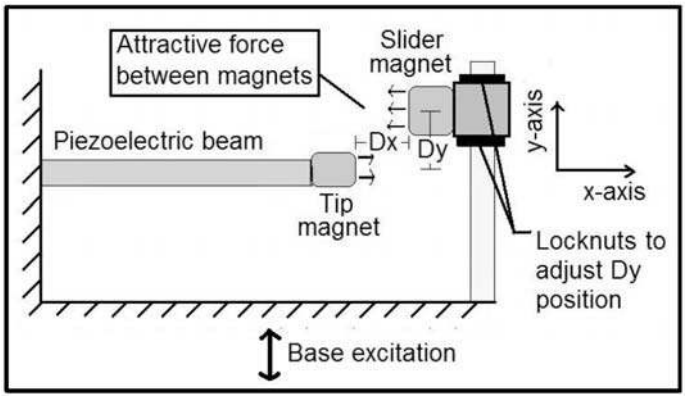

Figure 15 Schematic of the resonance tunable harvester (Reissman et al., 2009, copyright: SPIE)

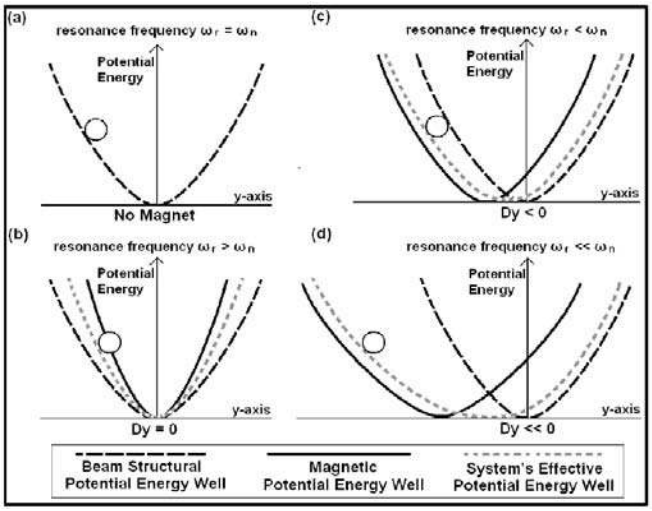

Figure 16 Qualitative hypothesis on varying sized potential energy wells with respect to the relative displacement of the magnets (Reissman et al., 2009, copyright: SPIE)

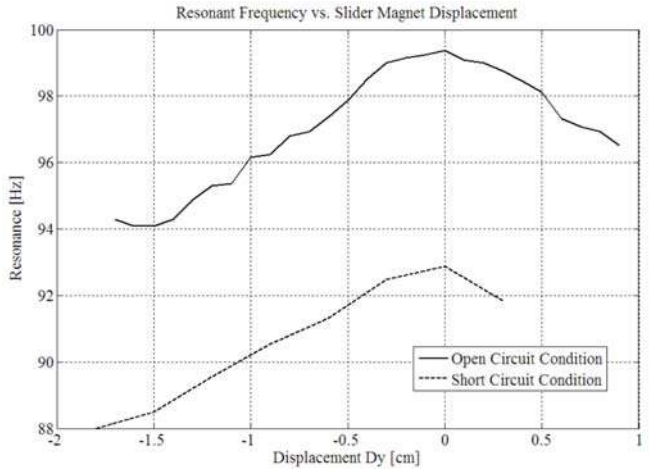

Figure 17 Open- and short-circuit frequencies with variable D_y (Reissman et al., 2009, copyright: SPIE)

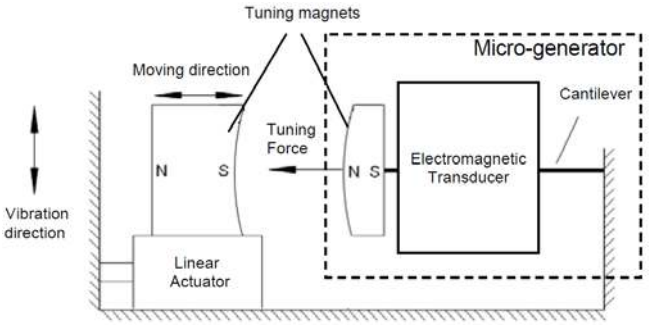

Figure 18 Schematic of the tuning mechanism (Zhu et al., 2008)

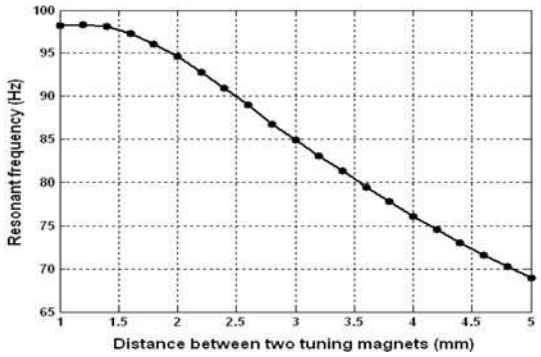

Figure 19 Resonance frequency versus distance between two magnets (Zhu et al., 2008)

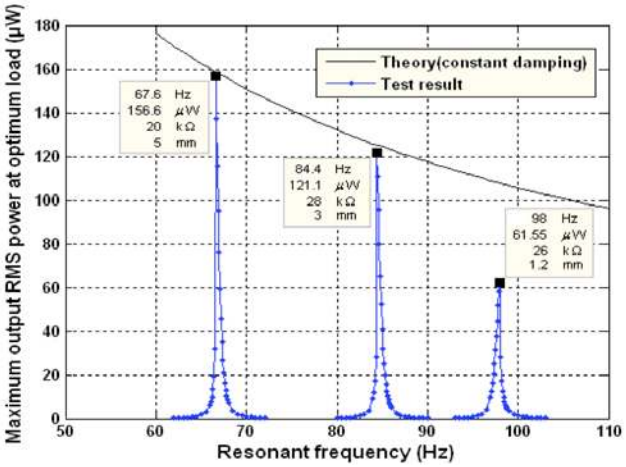

Figure 20 Maximum power output versus resonance frequency (Zhu et al., 2008)

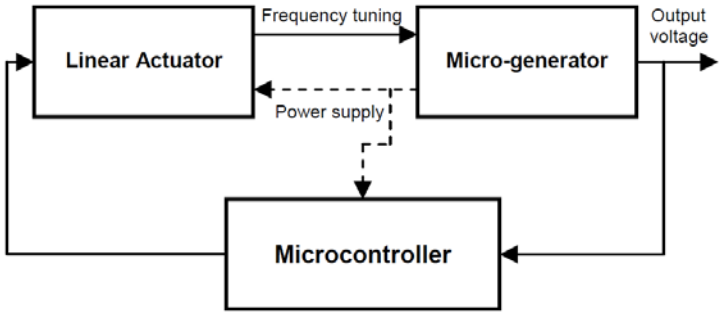

Figure 21 Block diagram of the closed loop tuning system (Zhu et al., 2008)

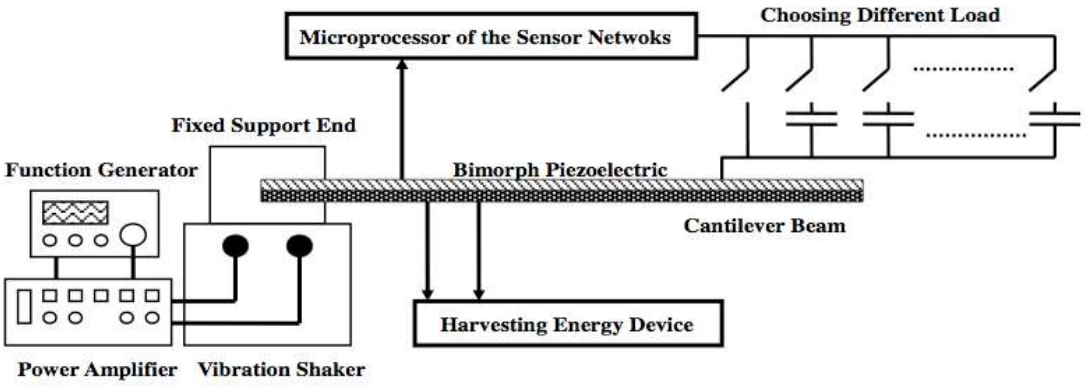

Figure 22 Experiment setup of the tunable energy harvesting system (Wu et al., 2006, copyright: SPIE)

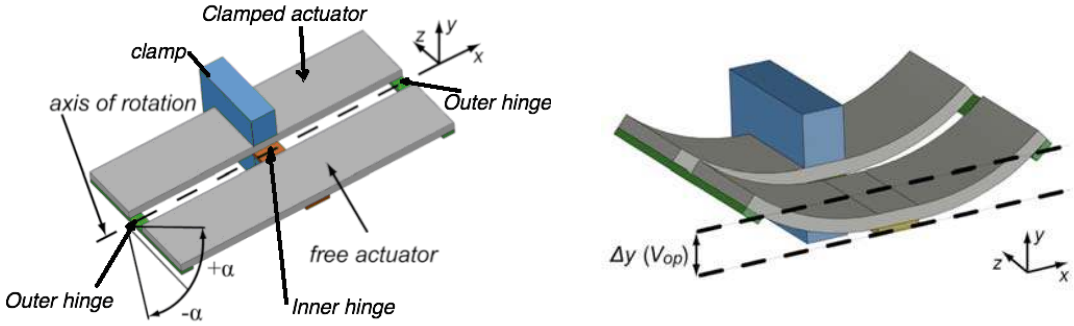

(a) (b)

Figure 23 (a) Tunable resonator with one clamped and one free actuator; (b) Both ends of the actuators are deflected by $\Delta y(V_{op})$ with applied tuning voltage (Peters et al., 2009, copyright: IOP Publishing)

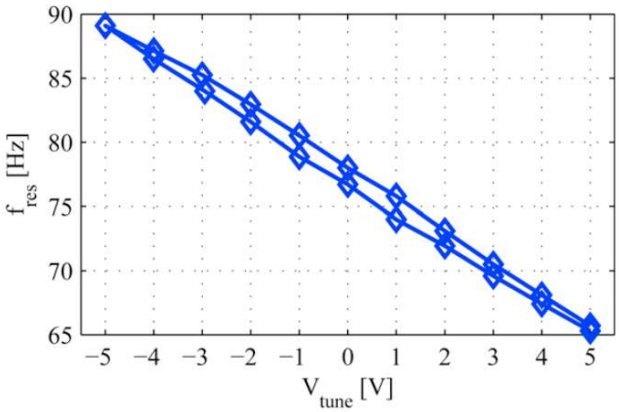

Figure 24 Measured resonance frequency versus applied tuning voltage (Peters et al., 2009, copyright: IOP Publishing)

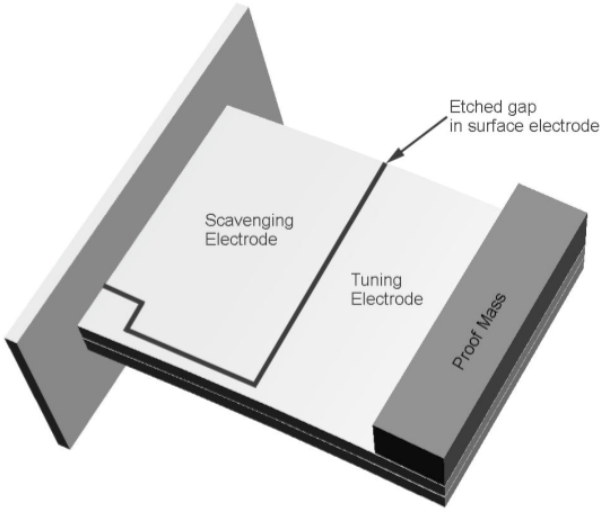

Figure 25 Schematic of a piezoelectric bender, in which, the surface electrode is etched to a scavenging and a tuning part (Roundy and Zhang, 2005, copyright: SPIE)

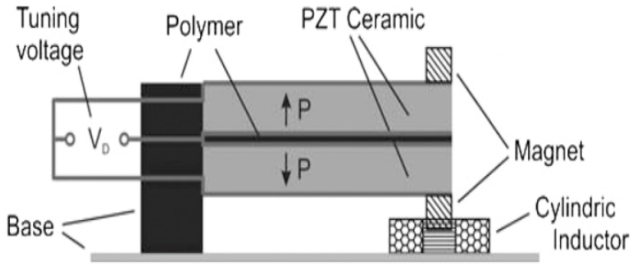

Figure 26 Schematic of the device (Wischke et al., 2010, copyright: IOP Publishing)

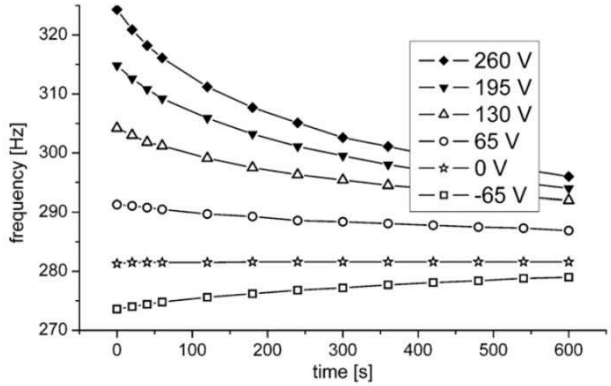

Figure 27 Time response of the harvester's operating frequency after disconnected control voltage (Wischke et al., 2010, copyright: IOP Publishing)

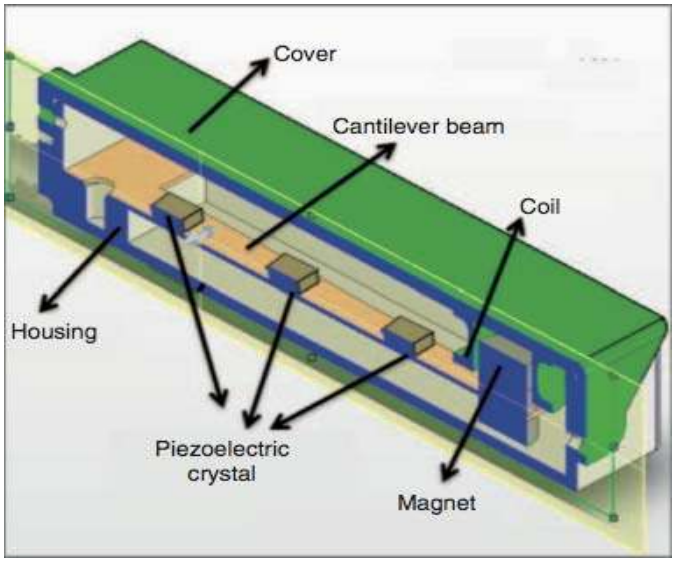

Figure 28 Schematic of the multimodal energy harvesting device (Tadesse et al., 2009, copyright: SAGE Publications)

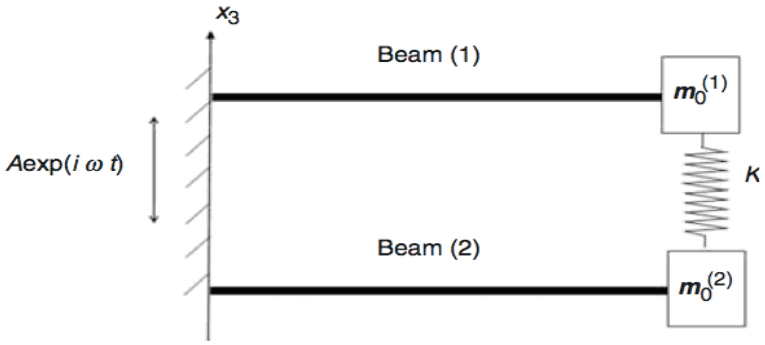

Figure 29 Schematic of two beams with two end masses elastically connected (Yang and Yang, 2009, copyright: SAGE Publications)

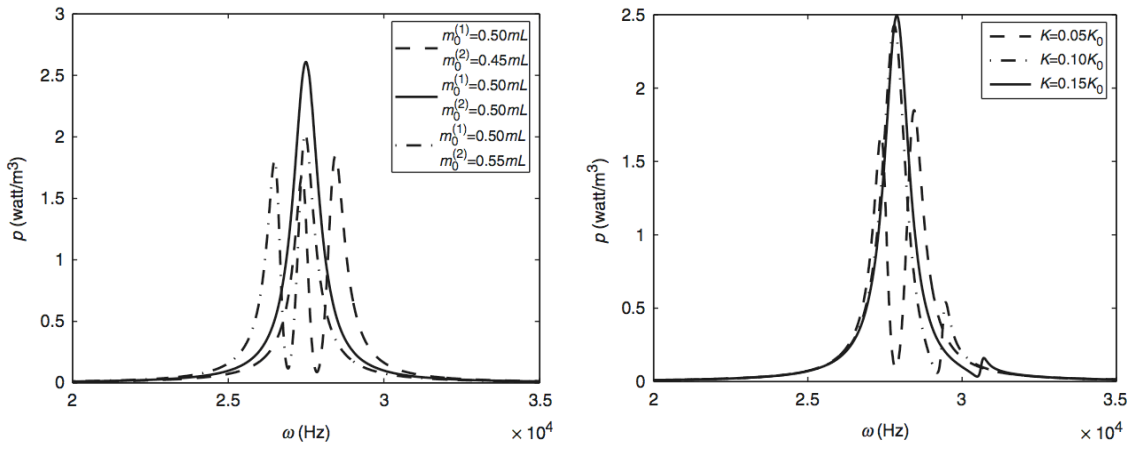

(a) (b)

Figure 30 Power density versus frequency for (a) different end mass pair with a fixed spring stiffness and (b) different spring stiffness with a fixed mass pair ($m_0^{(1)} \neq m_0^{(2)}$) (Yang and Yang, 2009, copyright: SAGE Publications)

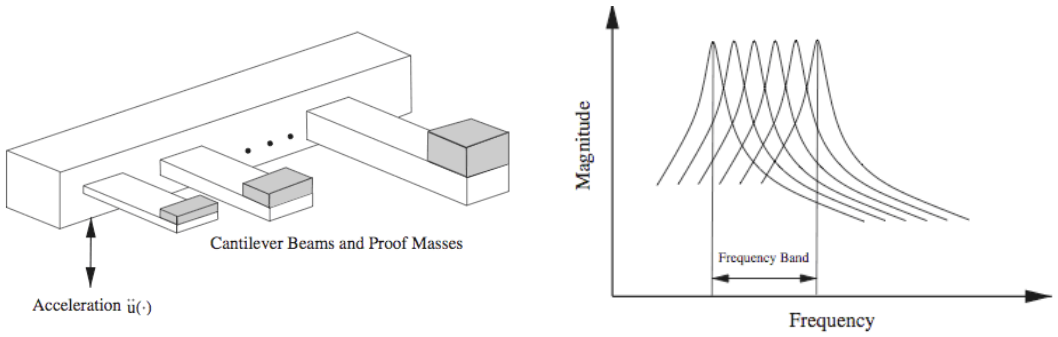

(a) (b)

Figure 31 (a) band-pass filter and (b) its transfer function (Shahruz, 2006a, copyright: Elsevier)

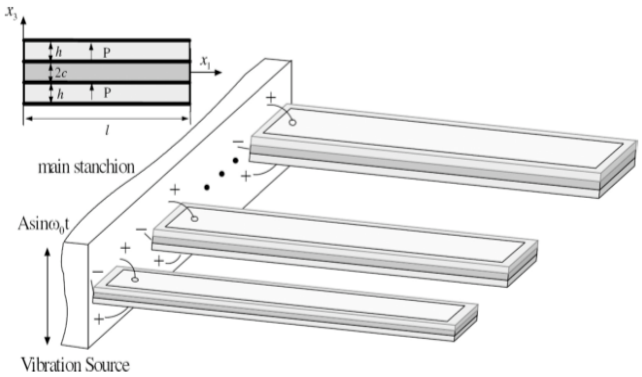

Figure 32 Schematic of the harvester with multiple PBs (Xue et al., 2008, copyright: IEEE)

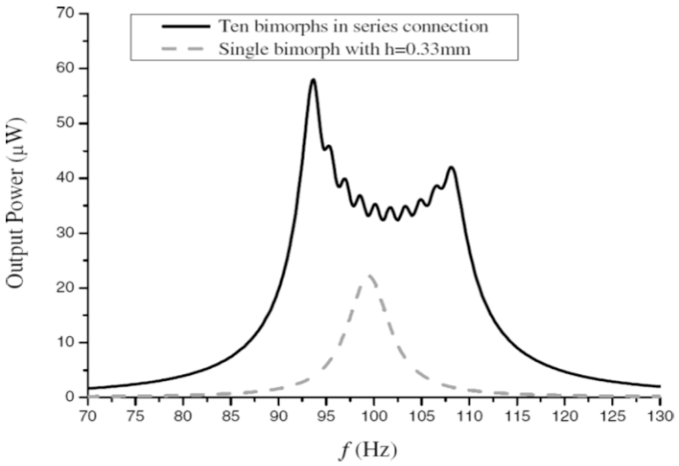

Figure 33 Power output versus frequency for 2 cases: a single PB and 10 PBs connected in series with various thicknesses (Xue et al., 2008, copyright: IEEE)

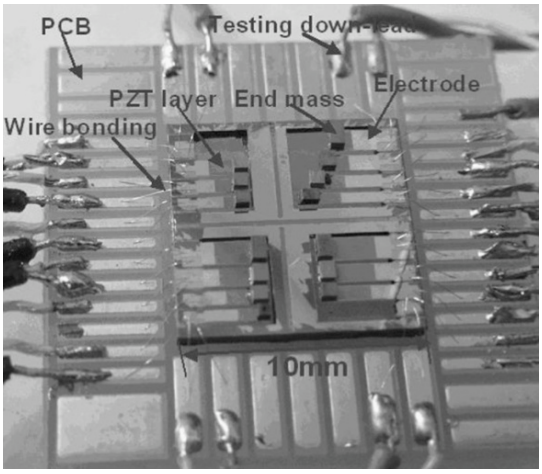

Figure 34 Schematic of the generator array prototype (Liu et al., 2008, copyright: Elsevier)

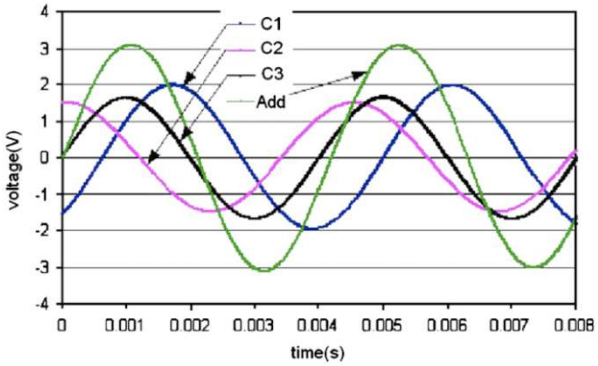

Figure 35 AC output of three cantilevers in an array and their direct serial connection (Liu et al., 2008, copyright: Elsevier)

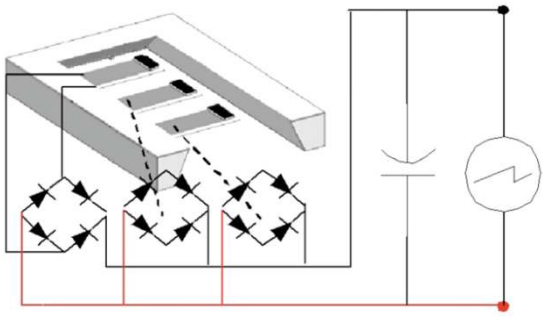

Figure 36 Electrical connection after AC–DC rectification (Liu et al., 2008, copyright: Elsevier)

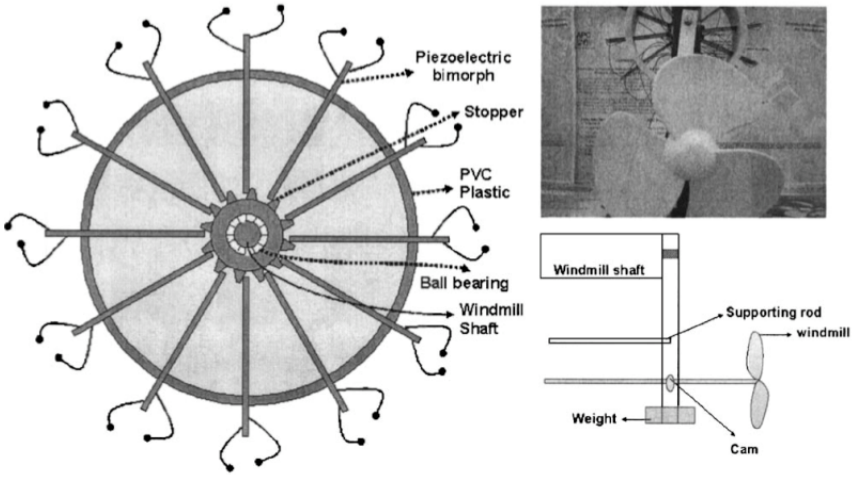

Figure 37 Schematic diagram of the piezoelectric windmill (Priya, 2005, copyright: American Institute of Physics)

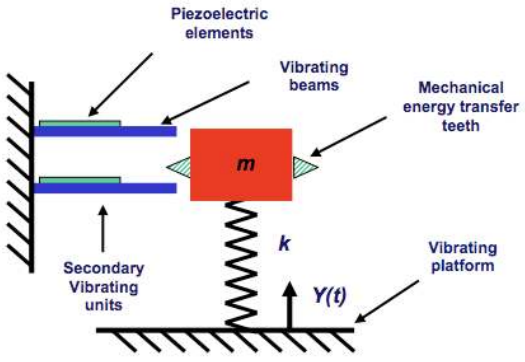

Figure 38 Schematic of the two-stage vibration energy harvesting design (Rastegar et al., 2006, copyright: SPIE)

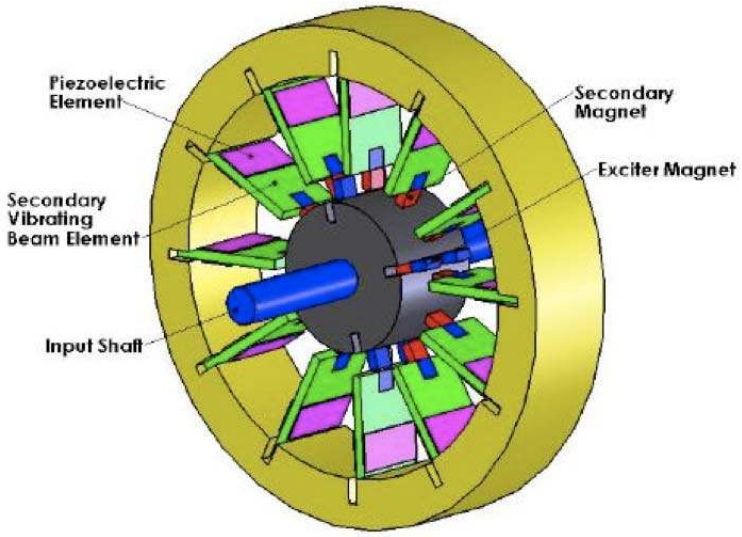

Figure 39 Two-stage rotary generator (Rastegar and Murray, 2009, copyright: SPIE)

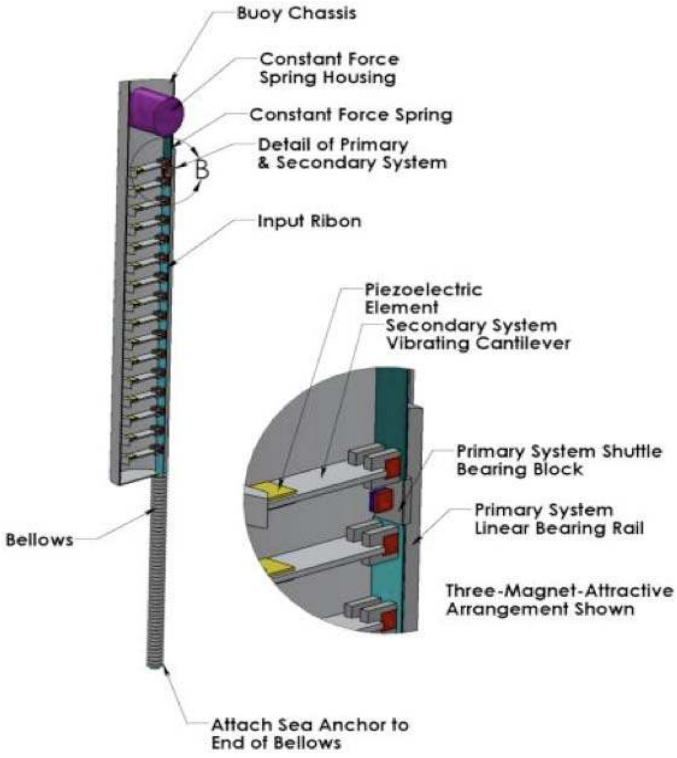

Figure 40 Two-stage linear generator for buoy (Murray and Rastegar, 2009, copyright: SPIE)

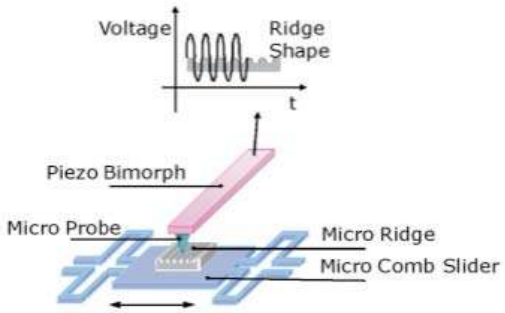

Figure 41 Concept of micro energy harvesting device using frequency up-conversion (Lee et al., 2007, copyright: IEEE)

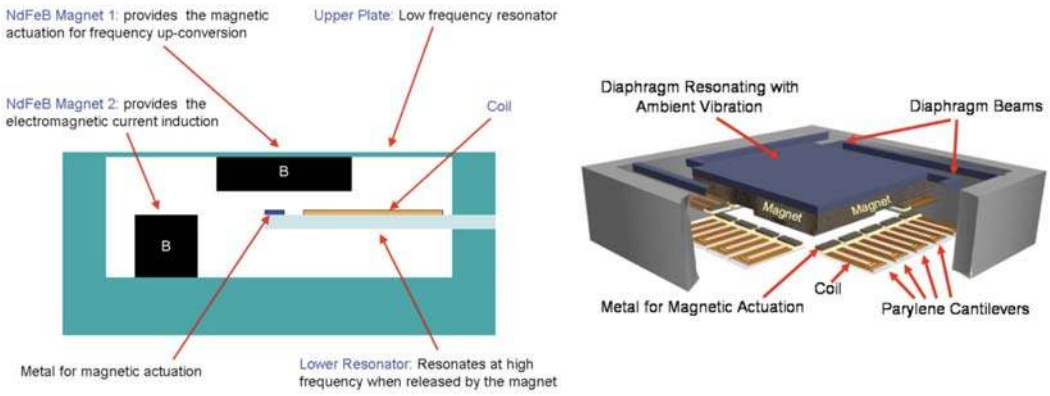

(a) (b)

Figure 42 Proposed microgenerator structure: (a) Simplified cross-sectional view. (b) 3-D view for microscale implementation (Kulah and Najafi, 2008, copyright: IEEE)

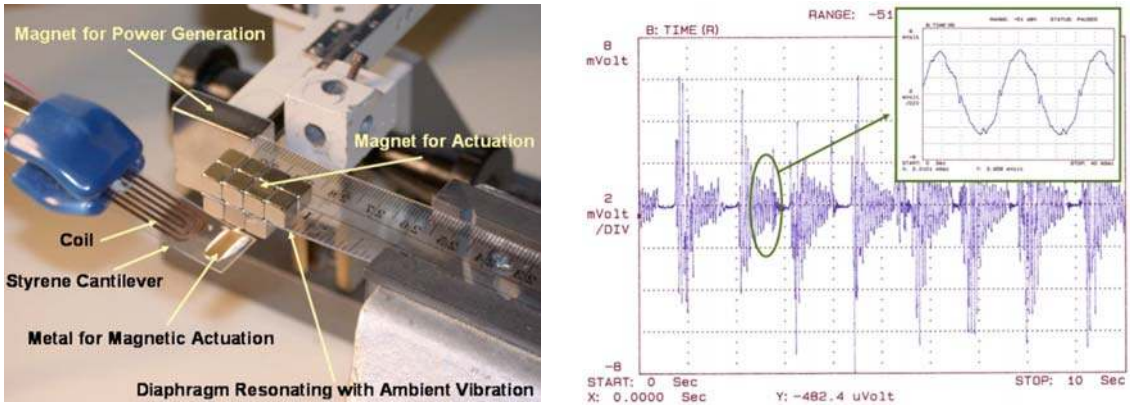

(a) (b)

Figure 43 (a) macroscale prototype for concept verification and (b) its measured voltage output (Kulah and Najafi, 2008, copyright: IEEE)

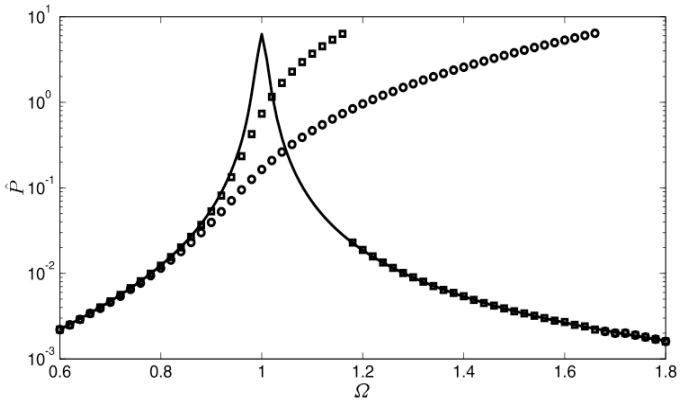

Figure 44 Numerical solution for non-dimensional power harvested with damping ratio ζ = 0.01 and excitation amplitude Y=0.5: Linear system (solid line), hardening system with nonlinearity b = 0.001 (□) and b = 0.01 (○) (b is the coefficient of the nonlinear term in Eqn. (7)) (Ramlan et al., 2010, copyright: Springer Science+Business Media)

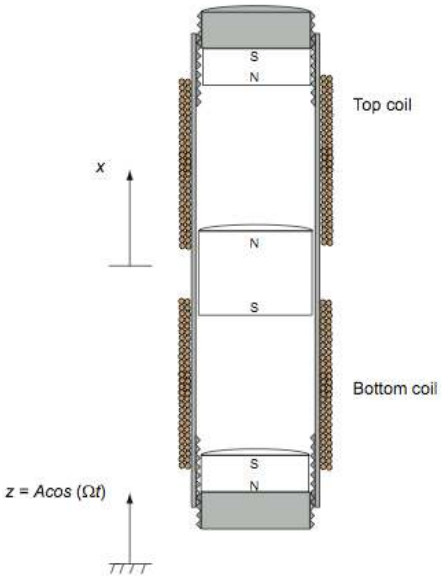

Figure 45 Schematic of the magnetic levetation system (Mann and Sims, 2009, copyright: Elsevier)

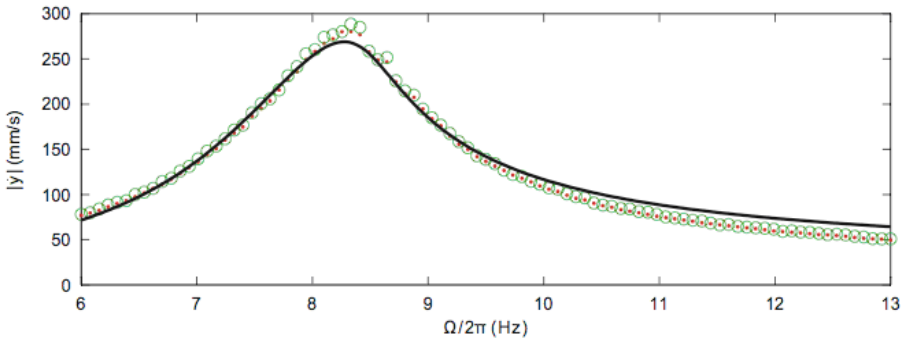

(a)

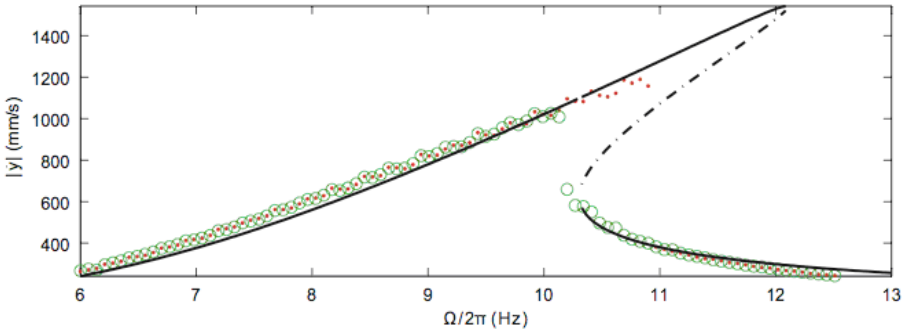

(b)

Figure 46 Experimental velocity response and theoretical predictions from forward (red dots) and reverse (green circles) frequency sweep under two excitation level: (a) 2.1m/s^2 and (b) 8.4m/s^2. Theoretical predictions include stable solutions (solid line) and unstable solutions (dashed line) (Mann and Sims, 2009, copyright: Elsevier)

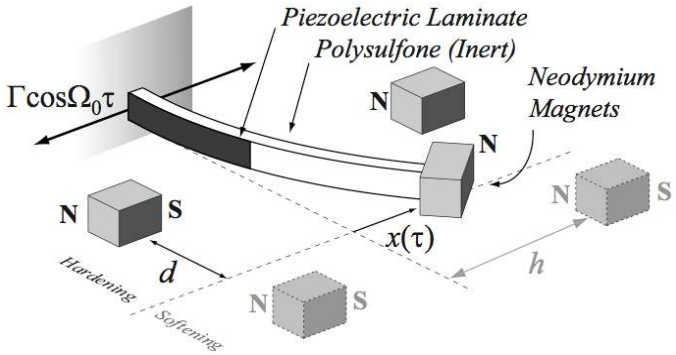

Figure 47 Schematic of the proposed nonlinear energy harvester (Stanton et al., 2009, copyright: American Institute of Physics)

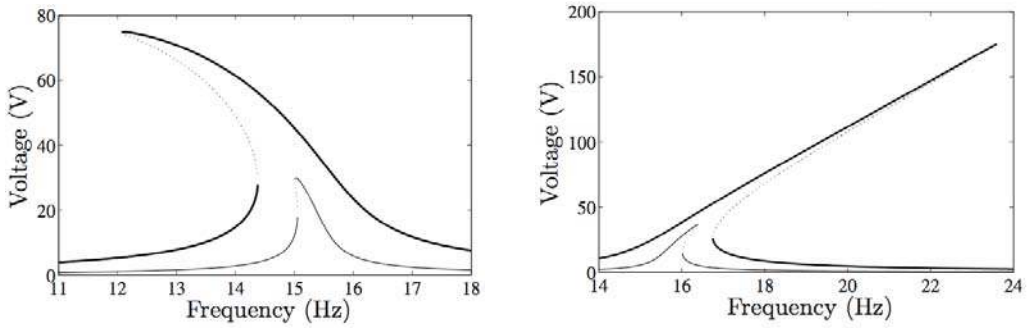

(a) (b)

Figure 48 Predicted response amplitudes of output voltage for (a) d = 5mm and (b) d = -2mm, corresponding to softening and hardening cases, respectively. Solid lines correspond to stable solutions while the dotted line to unstable solutions. The lighter line and darker line correspond to low and high excitation levels, respectively (Stanton et al., 2009, copyright: American Institute of Physics)

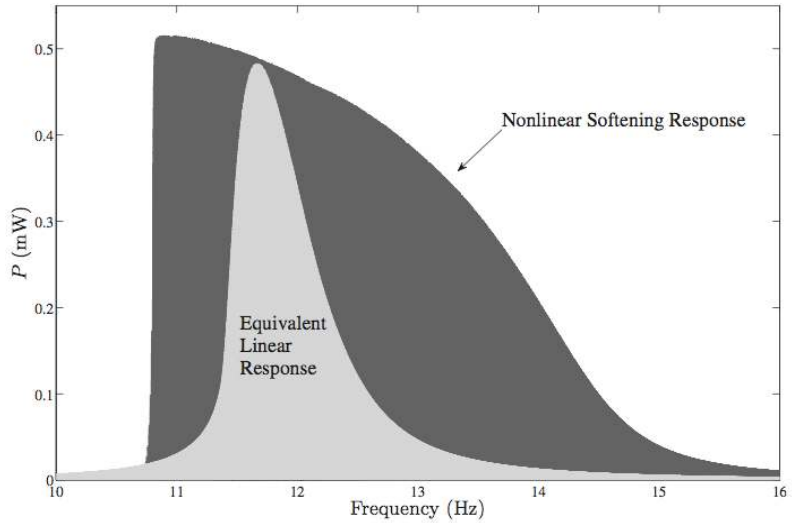

Figure 49 Comparison of the energy harvesting performances of nonlinear and linear configurations under the same excitation amplitude of 0.3g (Stanton et al., 2009, copyright: American Institute of Physics)

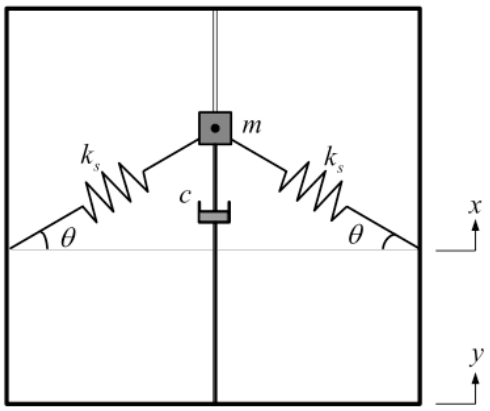

Figure 50 Arrangement of mass-spring-damper generator for the *snap-through* mechanism (Ramlan et al., 2010, copyright: Springer Science+Business Media)

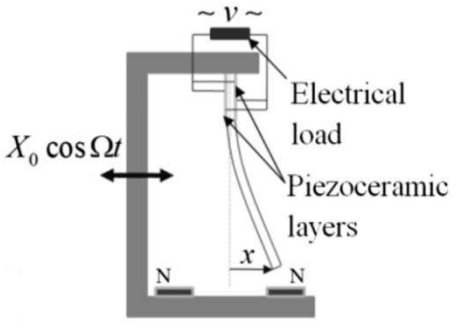

Figure 51 The piezomagnetoelastic generator (Erturk et al., 2009, copyright: American Institute of Physics)

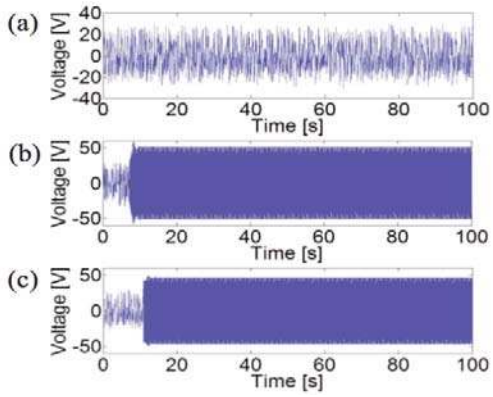

Figure 52 Experimental voltage histories: (a) Chaotic strange attractor motion (excitation: 0.5*g* at 8Hz); (b) Large-amplitude periodic motion due to the excitation amplitude (excitation: 0.8*g* at 8Hz); (c) Large-amplitude periodic motion due to a disturbance at t = 11s (excitation: 0.5*g* at 8Hz) (Erturk et al., 2009, copyright: American Institute of Physics)

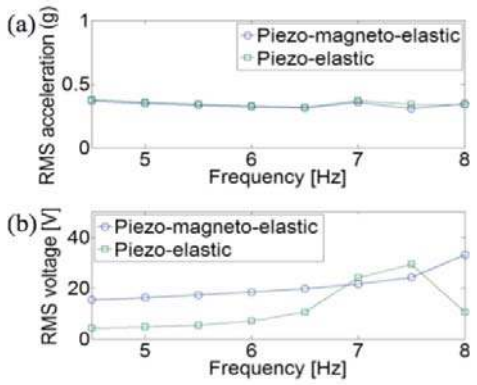

Figure 53 (a) Root mean square (rms) acceleration input at different frequencies (average value: 0.35*g*); (b) Open-circuit rms voltage output over a wide frequency range (Erturk et al., 2009, copyright: American Institute of Physics)

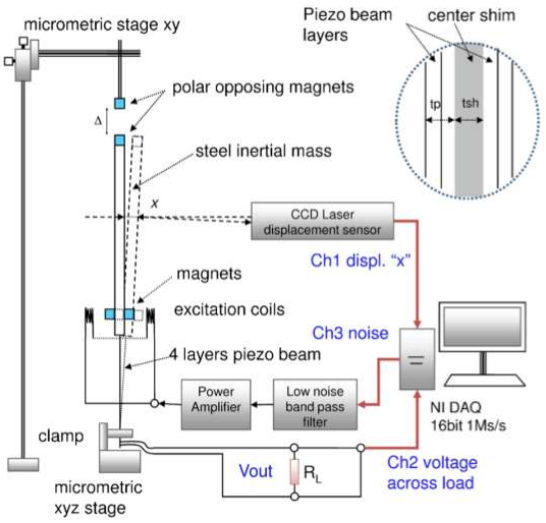

Figure 54 Schematic of the experimental apparatus (Cottone et al., 2009, copyright: American Physical Society)

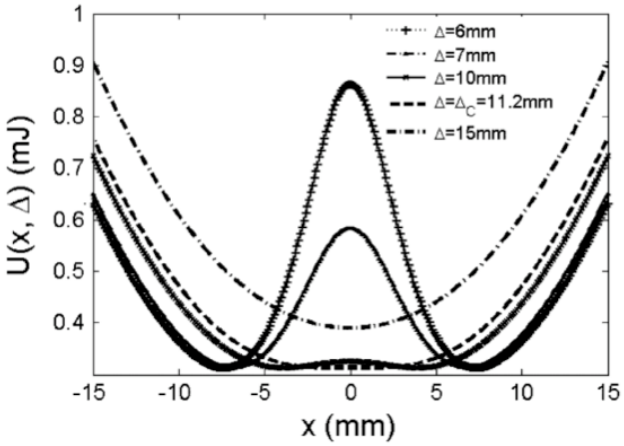

Figure 55 Inverted pendulum potential function $U(x)$ with different Δ (Cottone et al., 2009, copyright: American Physical Society)

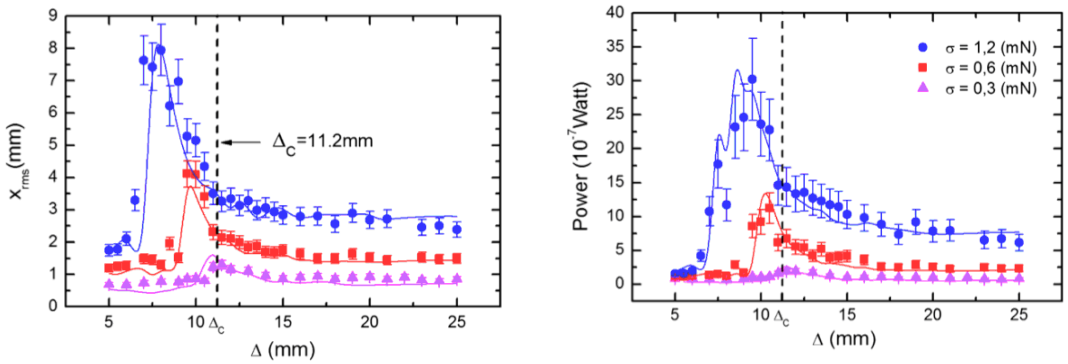

(a) (b)

Figure 56 (a) position x_{rms} and (b) power versus Δ for three different values of the noise standard deviation σ (Cottone et al., 2009, copyright: American Physical Society)

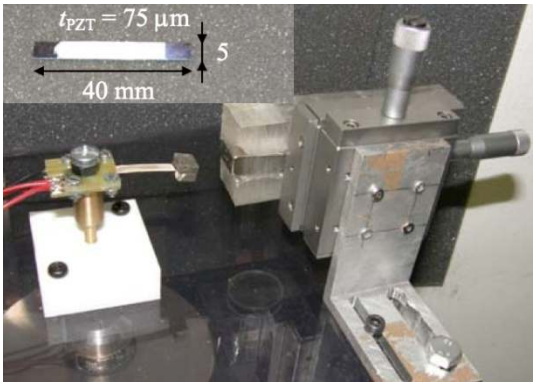

Figure 57 Experimental setup for the bistable system (Ferrari et al., 2009, copyright: Elsevier)

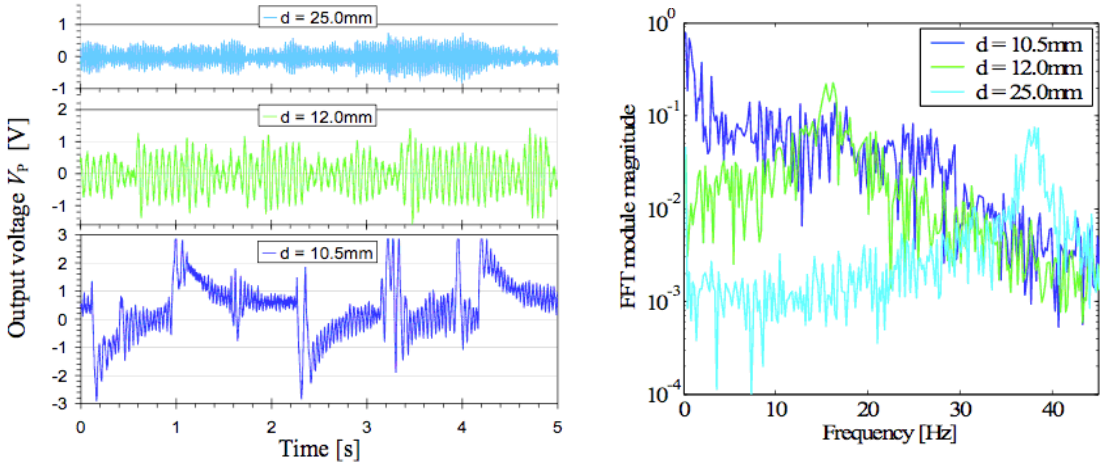

(a) (b)

Figure 58 (a) Output voltage from the piezoelectric cantilever beam and (b) its amplitude spectra measured for different distance between the magnets (Ferrari et al., 2009, copyright: Elsevier)

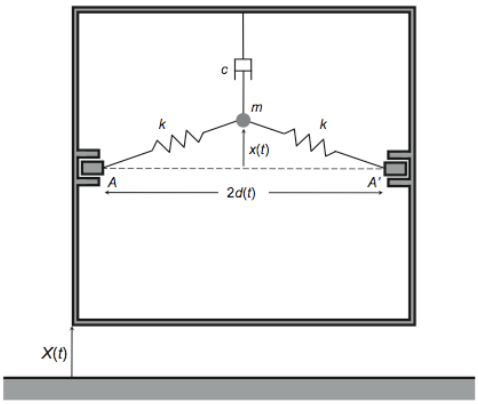

Figure 59 One degree-of-freedom beam model, in which the distance *A-A'* can be modulated at frequency ω (McInnes et al., 2008, copyright: Elsevier)

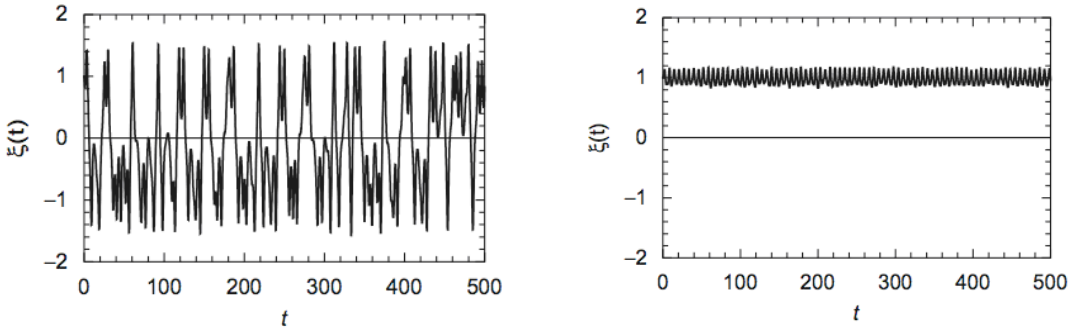

(a) (b)

Figure 60 Tuned system in stochastic resonance with $\omega = 1.2$: (a) response with forcing $\eta = 0.7$ and (b) response without forcing $\eta = 0$ (McInnes et al., 2008, copyright: Elsevier)